

Cite this: *Med. Chem. Commun.*, 2012, **3**, 1356

www.rsc.org/medchemcomm

REVIEW

## Diaryl ether derivatives as anticancer agents – a review

Florence Bedos-Belval,\* Anne Rouch, Corinne Vanucci-Bacqué and Michel Baltas

Received 18th July 2012, Accepted 7th September 2012

DOI: 10.1039/c2md20199b

This review article examines the diaryl ether scaffold found in natural products, related analogs and innovative molecules. It looks at encompassing synthesis, structure–activity relationships (SARs), and studies on biological action, namely in the context of anti-cancer activity. The aim of this review is to show that the diaryl ether scaffold is an invaluable structure for the design of anticancer drugs. It focuses essentially on work published from January 2000 to March 2012.

### 1. Introduction

Cancer is the main cause of death in economically developed countries and the second principal cause of death in developing countries.<sup>1</sup>

Cancer cells and normal cells have much in common in terms of the internal machinery enabling them to carry out all essential activities for survival. Chemotherapy drugs efficiently target processes that cancer cells need to grow and divide. Even if chemotherapy is particularly toxic to cancer cells, it also damages healthy cells. The use of standard chemotherapy unfortunately produces many severe side effects and the researchers' aim is to find an alternative free from side effects. The potent existing drugs also exhibit substantial limitations, such as low bioavailability, and (multi)drug resistance,<sup>2</sup> which henceforth encourage scientists to develop new agents as substitutes for chemotherapy.<sup>3</sup> Different biological processes can be targeted to overcome cancer and to classify the anti-cancer agents. We introduce here some of those targeted in the following review.

Apoptosis is mediated by a sequence of events that result in cell death. The action of classical anti-cancer drugs on tumor cell death is dependent on the induction of apoptosis.<sup>4</sup> In cancer cells, there is often an imbalance in favor of anti-apoptotic signals, which confers cells a resistance to chemotherapeutic drugs and radiation.<sup>5</sup> Bcl-2, a family of proteins, plays an important role in cancer-cell survival. In fact, Bcl-2 has been demonstrated to inhibit apoptosis by preventing the release of cytochrome C from mitochondria, thus preventing the activation of caspase-9 and caspase-3.<sup>6</sup> In the same way, the nuclear factor  $\kappa$ B (NF- $\kappa$ B) comprises a family of transcription factors involved in the regulation of a wide variety of biological responses. NF- $\kappa$ B regulates the expression of genes involved in many processes that play a key role in the development and progression of cancer such as proliferation, migration and apoptosis. Aberrant or

constitutive NF- $\kappa$ B activation has been detected in many human malignancies.<sup>7</sup> In a general way, pro-apoptotic drugs constitute an important class of anti-cancer agents.

One other promising biological target is the epidermal growth factor receptor (EGFR), because EGFR activation initiates a signaling cascade that leads to a number of processes involved in tumor progression, including increased proliferation, angiogenesis and invasion, and decreased apoptosis.<sup>8</sup> In addition, a variety of tumors express EGFR,<sup>9</sup> giving rise to the wide application of EGFR-targeted agents.

Cell growth and cell cycle pathways are activated in cancer cells. In the normal process, growth factors that are excreted by other cells bind to receptors on the cell surface, stimulating the cell to divide. Cancerous cells turn on the pathway in the absence of the growth factor. This may occur because of a mutation in a kinase or phosphatase gene. Protein kinases transmit signals to the nucleus through an intracellular cascade. The activity of kinases involved in transmission of proliferation signals in cancer cells often becomes more intense. Kinase inhibitors are generally small molecules designed to act with specificity on intracellular protein-kinases. Several new cancer treatments are designed to inhibit aberrantly activated kinases within cancer cells in an effort to prevent cell division.<sup>10a</sup> Another promising way to block cell growth is to prevent Ras-protein activation through inhibition of the farnesyl transferase. This enzyme attaches farnesyl groups to cysteine amino acids at the end of Ras-protein chains. By this way, Ras-proteins are able to anchor themselves to the inner surface of the cell membrane.<sup>10b</sup>

Like all cells, cancer cells require a constant supply of nutrients and oxygen in order to grow and divide. Tumors produce factors that stimulate the angiogenesis to provide them with food and oxygen to grow. One way to inhibit the development of blood vessels is to block the signals coming from the tumor.<sup>11a</sup>

The occurrence of simultaneous resistance against different drugs (MDR) is a major problem in the treatment of cancer with chemotherapy. The most common mechanism of multidrug resistance is the export of drugs from the cell by means of ATP-Binding Cassette (ABC) transporters. ABC transporters are

Laboratoire de Synthèse et Physico-Chimie de Molécules d'Intérêt Biologique, Université P. Sabatier, bat 2R1, 118 Route de Narbonne, 31062 Toulouse Cedex 9, France. E-mail: bedos@chimie.ups-tlse.fr; Fax: +33 (0)5 615 56011; Tel: +33 (0)5 615 56800

proteins that span throughout the cell membrane and can actively transport compounds. The affinity of this protein to a broad range of substrates makes it able to transport many of the drugs of chemotherapies but at the same time it makes it susceptible towards various inhibitors.<sup>11b</sup>

The degradation of the extracellular matrix that surrounds all cells is an important process in the formation of new blood vessels. Growing blood vessel cells secrete enzymes called matrix metalloproteinases (MMPs) that are able to digest the extracellular matrix and allow blood vessels to invade the area and supply a tumor with nutrients. Inhibition of this process is the target of several drugs.<sup>12</sup>

Microtubules are extremely important in the process of mitosis, during which the duplicated chromosomes of a cell are separated into two identical sets before cleavage of the cell into two daughter cells. Their importance in mitosis and cell division makes microtubules an important target for anti-cancer drugs.<sup>13</sup> Microtubules and their dynamics are the targets of a chemically diverse group of anti-mitotic drugs (with various tubulin-binding sites) that have been used with great success in the treatment of cancer. Interestingly, a large number of chemically diverse substances bind to soluble tubulin and/or directly to tubulin in the microtubules. Most of these compounds are anti-mitotic agents and inhibit cell proliferation by acting on the polymerization dynamics of spindle microtubules, the rapid dynamics of which are essential for proper spindle function.<sup>14</sup> The microtubule-destabilizing agents inhibit microtubule polymerization at high concentrations and include several compounds such as the *Vinca* alkaloids, cryptophycins, halichondrins, estramustine, colchicine and combretastatins. Because cancer cells divide more than normal ones, they are vulnerable to mitotic poisoning.

Although chemotherapy is the mainstay of cancer therapy, the use of available chemotherapeutics is often limited mainly due to undesirable side effects and a limited choice of available anti-cancer drugs. This clearly underlies the urgent need for developing novel chemotherapeutic agents with more potent anti-tumor activities.

Diaryl ethers are frequently found in substructures of many biologically important natural products.<sup>15,16</sup> Diaryl ethers can be commonly synthesized *via* three general ways which include Ullmann ether synthesis,<sup>17</sup> Buchwald Pd-catalyzed ether synthesis<sup>18</sup> and aromatic nucleophilic substitution (S<sub>N</sub>Ar) based addition reactions.<sup>19</sup> In this report, we focus on the diaryl ether skeleton in the chemical structure of anti-cancer agents, its chemical synthesis, potent activities and biological targets.

## 2. Natural and non-natural diaryl ethers

### 2.1. Obovatol and analogs

Obovatol (Fig. 1) is a neolignan isolated from *Magnolia obovata* bark which has been used for ages in folk medicine for gastrointestinal disorders. This active component has various pharmacological properties such as anti-oxidant, anti-platelet,<sup>20</sup> anti-inflammatory<sup>21</sup> and anti-tumor activities.<sup>22</sup>

Lee and co-workers (2008) have studied obovatol expecting activity on colorectal cancer.<sup>23</sup> *In vivo* studies on a SW620 tumor xenograft model of nude mice injected intraperitoneally with obovatol (5 mg kg<sup>-1</sup> d<sup>-1</sup>, diluted in 0.5% Tween 80) showed a

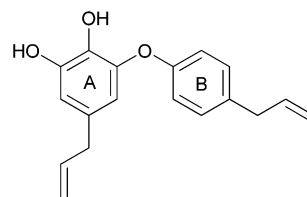


Fig. 1 Chemical structure of obovatol.

50% decrease in tumor volume ( $277.0 \pm 54 \text{ mm}^3$  in the obovatol treatment group *versus*  $554.4 \pm 63 \text{ mm}^3$  in the control group after 21 days of treatment). As shown in Table 1, obovatol inhibited the growth of SW620 cells in a dose-dependent and time-dependent manner. Further experiments (data not shown here) suggested that obovatol induced apoptosis.

Obovatol appears to be an interesting frame to design derivatives with anti-tumor properties. So, J.-H. Kwak and co-workers<sup>24</sup> have proposed a short total chemical synthesis of obovatol based on chemoselective *ortho*-bromination and copper-catalyzed coupling (Scheme 1).

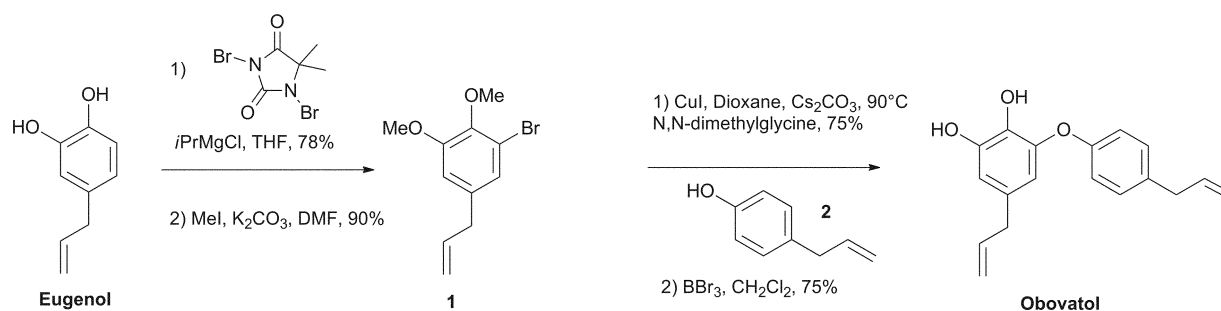
Eugenol was brominated by using *i*-PrMgCl as a base and 1,3-dibromo-5,5-dimethylhydantoin as an electrophile to give predominantly the brominated compound in 78% yield after optimization. Further methylation led to molecule **1**. A diaryl ether skeleton was formed by the Ullmann modified coupling reaction using copper iodide, in the presence of cesium carbonate as a base, *N,N*-dimethylglycine as a ligand and 4-allylphenol **2** in dioxane at 90 °C. The corresponding diaryl ether obtained with 75% under these specific conditions was demethylated under Lewis acid conditions to give the expected obovatol.

M.-S. Lee *et al.*<sup>25</sup> (2007) have synthesized analogs starting from methyl gallate arguing that the gallic unit is structurally close to the A-ring of obovatol (see Fig. 1) and present in (–)-epigallocatechin gallate, an anti-cancer agent.<sup>26</sup> After demethylation of phenolic hydroxy functions under classical conditions, the resulting phenol **3** has been engaged in a coupling reaction with a variety of arylboronic acids **4** under Evans conditions (Scheme 2).<sup>27</sup>

The synthesized diaryl ethers **5** have been screened for their NF-κB luciferase activities in prostate LNCaP and colon cancer HCT 116 cells, respectively. The transcription factor NF-κB cell survival stimulated by the induction of genes coding for anti-apoptotic proteins<sup>28</sup> is abnormally active in many solid tumors and as such represents a potential therapeutic target. NF-κB luciferase assay showed that phenol functionality was essential for inhibition properties. Moreover, compounds **5a** and **5g** bearing 4-halogen of ring B exhibited the best inhibition activities in the same range as obovatol itself. These data shed light on the structural requirements for anti-tumor activity.

Table 1 Effect of obovatol (expressed in % of cell inhibition) on the growth of SW620 cells

Concentration (μM)	30	50	100
Time (h) 24	7 ± 1.1	21 ± 0.3	36 ± 0.07
48	26 ± 0.3	57 ± 0.5	92 ± 0.05
72	33 ± 1	64 ± 0.2	97 ± 0.01
96	18 ± 1	85 ± 0.1	98 ± 0.01



Scheme 1 Total synthesis of obovatol.

## 2.2. Depsidones and analogs

Lichens are the symbiotic organisms of fungi and algae distributed worldwide.<sup>29</sup> Lichens accumulate large concentrations of products, particularly aromatic phenolic compounds, sometimes exceeding 20% of dry weight. The majority of these compounds originate from the fungi. Lichen extracts have been used for ages in folk medicines.<sup>30</sup> Depsidones, cyclic diaryl ethers with an ester link joining the two aromatic rings, have been isolated commonly from various lichens.<sup>31</sup> A large variety of aryl substitutions is observed according to the different lichen sources. We focus here on natural depsidone extracted from a lichen, *Diploicia canescens*.

Millot and co-workers<sup>32</sup> (2009) have isolated and confirmed the chemical structure of depsidones **6**, **7** and **8** (Fig. 2). Their cytotoxic effects against B16 murine melanoma and HaCaT human keratinocyte cell lines were evaluated using the MTT assay, with etoposide (topoisomerase II inhibitor used as a cancer drug) with positive control ( $IC_{50} = 0.28$  and  $0.55 \mu M$  for B16 and HaCaT, respectively) (Table 2). The tested compounds showed significant and selective cytotoxicity against B16 cells when compared to HaCaT cells. The most cytotoxic effect is the non-chlorinated depsidone **8**.

In the same year, the research group of Chomcheon<sup>33</sup> isolated depsidones **9–12** and diaryl ether **13** from endophytic fungus *Corynespora cassicola* L36 to discover new bioactive substances against aromatase (Fig. 3). The enzyme aromatase is always present in or around breast cancer tumor,<sup>34</sup> and is hence becoming an interesting target for potential drugs.

Only corynesidone A (**9**) acted as an aromatase inhibitor with an  $IC_{50}$  value of  $5.3 \mu M$  (ref. 35) close to that of aminoglutethimide, a first generation aromatase inhibitor drug.

A weak cytotoxic activity has been measured against different cancer cell lines (HeLa, cervical adenocarcinoma cell line; HuCCA-1, human lung cholangiocarcinoma cancer cells; HepG2, human hepatocellular liver carcinoma cell line; T47D, human mammary adenocarcinoma cell line; MDA-MB231, human breast cell line; S102, human liver cancer cell line; A549,

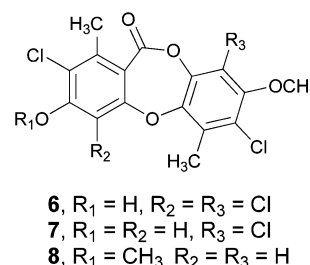
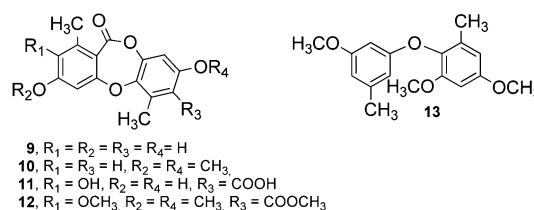
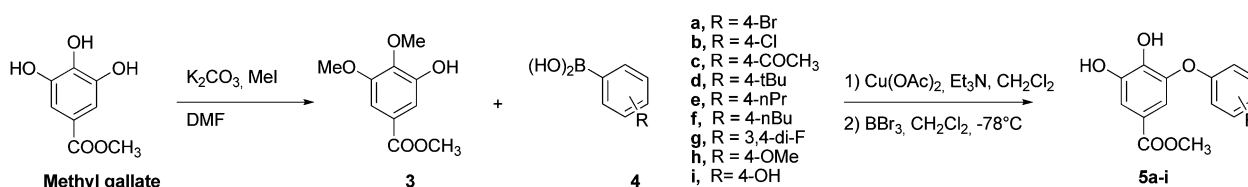
Fig. 2 Depsidones structures isolated from *Diploicia canescens*.

Table 2 Cytotoxic activities against B16 murine melanoma cells and HaCaT human keratinocyte cells

Cell lines	$IC_{50}$ ( $\mu M$ )			
	<b>6</b>	<b>7</b>	<b>8</b>	Etoposide
B16	$4.0 \pm 1.0$	$1.7 \pm 0.2$	$0.4 \pm 0.1$	$0.28 \pm 0.08$
HaCaT	>10	$4.3 \pm 0.8$	$6.1 \pm 0.6$	$0.55 \pm 0.15$

Fig. 3 Structures of isolated depsidones and diaryl ether from *Corynespora cassicola* L36.

human lung carcinoma cell line; HL-60, human promyelocytic leukemia cell line; and MOLT-3, T-lymphoblast (acute lymphoblastic leukemia)) for all depsidones **9–12** making them not interesting as potential drug candidates (Fig. 3). Diaryl ether



Scheme 2 Synthesis of obovatol derivatives.

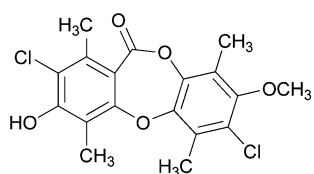


Fig. 4 Chemical structure of vicanicin.

**13** exhibited moderate cytotoxicity (HL-60  $IC_{50}$  = 2.2  $\mu$ M, MOLT-3  $IC_{50}$  = 1.4  $\mu$ M) when compared to etoposide (HL-60  $IC_{50}$  = 0.61  $\mu$ M, MOLT-3  $IC_{50}$  = 0.02  $\mu$ M).

The aromatase inhibitor activity of corynesidone A (**9**) does not result in any expected cytotoxic properties. Despite these not so very convincing results, research on lichen metabolites as potent anti-tumor agents is going on. In 2012, Russo *et al.*<sup>36</sup> have established that the depsidone vicanicin (Fig. 4) isolated from lichen is able to inhibit growth of prostate cancer cells. Prostate cancer, one of the most common cancers, is often curable by conventional therapy.<sup>37</sup> However, recurrent prostate cancers are being quite frequent,<sup>38</sup> the development of more effective cancer treatments requiring new and innovative drugs is consequently still of utmost importance.

Table 3 Chemical structure and cytotoxicity of rhuschalcones **14–17**

	ED <sub>50</sub> <sup>a</sup> ( $\mu$ g mL <sup>-1</sup> )			
Cell lines	<b>14</b>	<b>15</b>	<b>16</b>	<b>17</b>
Colo 205	11	15	4	23 <sup>b</sup>
HCT 116	5	15 <sup>b</sup>	5	<sup>b</sup>
HCT 15	51	<sup>b</sup>	4	<sup>b</sup>
HT 29	3	14	3	<sup>b</sup>
KM 12	17	19 <sup>b</sup>	4	<sup>b</sup>
SW 620	42	<sup>b</sup>	3	<sup>b</sup>

<sup>a</sup> ED<sub>50</sub>: median effective dose that produces the cytotoxic effect in 50% of treated cells. <sup>b</sup> Not reached at the tested concentration.

Vicanicin has been demonstrated to be cytotoxic against androgen-insensitive DU-145 cells and androgen-sensitive LNCaP cells in dose–response relationships (from 6.5  $\mu$ M to 50  $\mu$ M). This depsidone has revealed no cytotoxic effect on normal human non-immortalized buccal fibroblast (BFC). This selectivity has prompted further studies. Vicanicin has been shown to inhibit apoptosis by increasing caspase-3 activity, a cytosolic cysteine-protease implicated in the enzymatic cascade of apoptosis. Vicanicin has been suggested to equally reduce heat shock protein Hsp70 (suspected to participate in resistance to chemotherapy) levels thus inducing cell death by an intrinsic or mitochondrial apoptotic pathway.

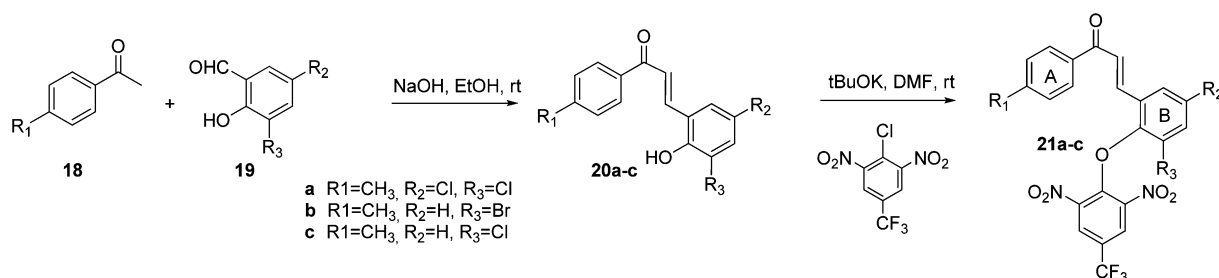
### 2.3. Chalcone derivatives

Chalcones possess a 1,3-diaryl-2-propenone skeleton. They are intermediates in biosynthesis of flavonoids which are widespread substances present in plants. Chalcones have exhibited various inhibition effects on cell proliferation and have demonstrated anti-cancer activities.<sup>39</sup> In general natural bichalcones carry either C–O–C or C–C linkage between the two chalcone units. It is noted that bichalcones with diaryl ether link are rare in nature. Focusing on this class of bichalcones named Rhuschalcones by the group of Abegaz,<sup>40</sup> some of them isolated from *Rhus pyroides* have demonstrated various degrees of cytotoxicity on different cancer cell lines. Rhuschalcones have shown better selectivity regarding colon cancer cell lines,<sup>41</sup> especially the HT29 and HCT-116 cell lines (Table 3). The most potent cytotoxic agent is bichalcone **16**.

In the field of anti-cancer lead drugs development, the bichalcones should be selected as the synthetic targets for the preparation of cytotoxic agents.

Recently, new chalcones including a diaryl ether moiety have been designed and synthesized as anti-tubulin agents. Zhang *et al.*<sup>42</sup> (2007) have introduced nitrophenyl and trifluoromethyl groups *via* ether linkage to a chalcone skeleton in order to improve anti-cancer and anti-tubulin activities. Diaryl ether chalcones derivatives have been prepared starting from substituted acetophenone **18** and salicylaldehyde **19a–c** under basic conditions. Then aromatic nucleophilic substitution has occurred to give the corresponding derivatives **21a–c** (Scheme 3).

The potent anti-cancer activity of derivatives **21a–c** has been evaluated on two cell lines: MCF-7, a human breast cancer cell line and A549, an adenocarcinomic human alveolar basal epithelial cell line.  $IC_{50}$  has been determined by an MTT (3-(4,5-dimethylthiazol-2-yl)-2,5-diphenyltetrazolium bromide) test. Moreover, anti-tubulin polymerization effects have been tested with purified bovine brain tubulin. Colchicine indicated in the



Scheme 3 General preparation of diaryl ether chalcone derivatives.



**Table 4** Anti-proliferative activity of diaryl ether chalcones **3a–c** on MCF-7 and A549 and anti-tubulin polymerization activity

Compound	A ring			B ring			IC <sub>50</sub> (μg mL <sup>-1</sup> )		
	R <sub>1</sub>	R <sub>2</sub>	R <sub>3</sub>				MCF-7	A549	Tubulin
<b>21a</b>	CH <sub>3</sub>	Cl	Cl				0.70 ± 0.02	10.05 ± 0.23	4.87 ± 0.21
<b>21b</b>	CH <sub>3</sub>	H	Br				0.55 ± 0.01	6.85 ± 0.42	6.41 ± 0.10
<b>21c</b>	CH <sub>3</sub>	H	Cl				0.03 ± 0.002	0.95 ± 0.04	1.42 ± 0.06
Colchicine							0.51 ± 0.06	0.74 ± 0.08	1.70 ± 0.12
CA-4							0.43 ± 0.04	0.53 ± 0.04	0.81 ± 0.08

treatment of cancers (for its anti-mitotic properties) and combrestatin A-4 (CA-4), a potent cancer cell growth inhibitor binding to tubulin, has been used as a reference during the biological tests. A few more potent anti-proliferative activities are summarized in Table 4.

These results have proved a structure–activity relationship. The substitution on aromatic rings A and B has also been demonstrated to play a crucial role in the expected biological properties. IC<sub>50</sub> is lower with A ring substituted by an electro-donating group like a methyl one. B-ring substitution is also important for the anti-cancer effects. The addition of one halogen on B ring ensures higher anti-cancer activity. These diaryl ether chalcones have shown more interesting anti-proliferative effects on MCF-7 cells. Derivative **21c** is the most potent of the series with (IC<sub>50</sub> = 0.03 μg mL<sup>-1</sup> for MCF-7 and IC<sub>50</sub> = 0.95 μg mL<sup>-1</sup> for A549), comparable to the positive control colchicine (IC<sub>50</sub> = 0.51 μg mL<sup>-1</sup> for MCF-7, IC<sub>50</sub> = 0.74 μg mL<sup>-1</sup> for A549, respectively). Furthermore, flow cytometry assays have shown that diaryl ether **21c** (5 μg mL<sup>-1</sup> for 24 h) has induced cell cycle arrest at G2/M for 67.93% of these cells. Molecular docking studies with tubulin (PDB code: 1SA0, LigandFit Dock protocol of Discovery Studio 3.1.) have demonstrated that compound **21c** is bound to the colchicine binding site of tubulin *via* hydrophobic interactions, hydrogen bond and one π-cation interactions.<sup>42</sup> Thus, agent **21c** anti-proliferative activities could be related to its anti-tubulin polymerization effect suggesting that bichalcone diaryl ether is a potential skeleton for further new anti-cancer drug design.

## 2.4. Non-natural based diaryl ethers

**2.4.1. Combrestatin analogs.** Combretastatin A-4, a natural product isolated from the bark of the African bush willow

*Combretum caffrum*, has been found to strongly inhibit the polymerisation of tubulin by binding to the colchicine site.<sup>43</sup> Combretastatin A-4 is also able to elicit selective and irreversible vascular shutdown within solid tumours, leaving normal vascular tissues intact.<sup>44</sup> These anti-cancer properties make combretastatin A-4 a really valuable lead in the search for new synthetic analogs.<sup>45</sup> In this area, N. J. Lawrence *et al.*<sup>46</sup> (2001) synthesized diaryl ether analogs of combrestatin A-4 replacing the ethylene linkage by an ether one to evaluate its importance on the anti-cancer properties.

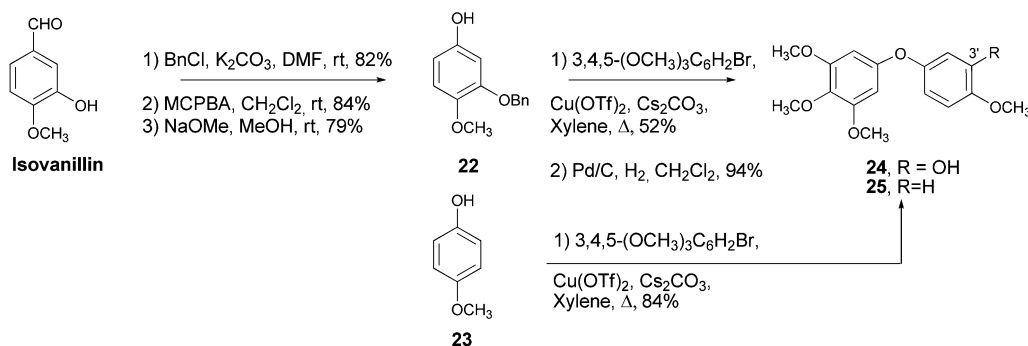
Benzyl-protected isovanillin was submitted to a sequential Baeyer–Villiger oxidation followed by ester methanolysis giving rise to phenol **22** (Scheme 4). Diaryl ether **24** was obtained under Buchwald coupling conditions<sup>47</sup> in the presence of 3,4,5-trimethoxybromobenzene and copper triflate, followed by a hydrogenolysis step. Compound **24** was obtained under the same coupling conditions starting from phenol derivative **23**.

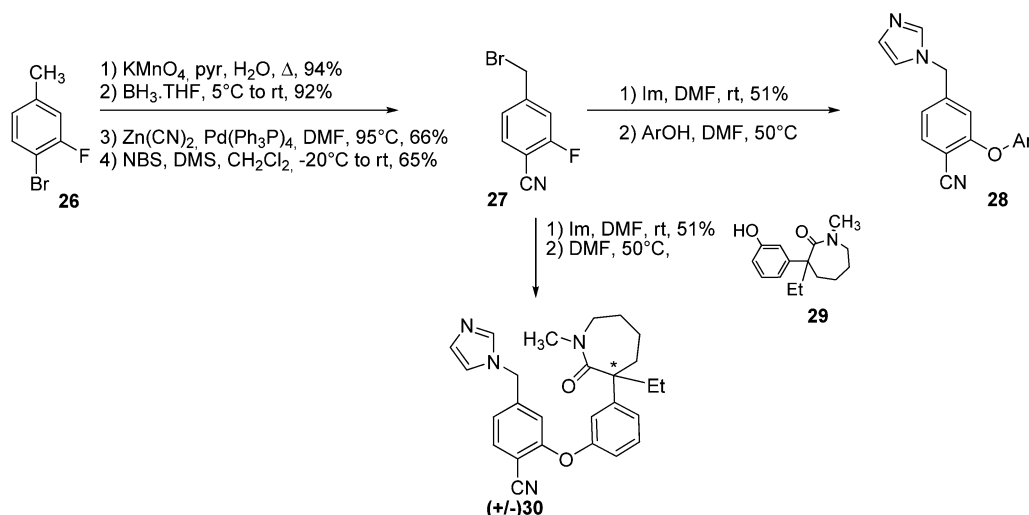
Diaryl ether **24** clearly inhibits the K562 human erythromyeloblastoid leukemia cell growth (IC<sub>50</sub> = 50 nM) when compared to diaryl ether **25**, demonstrating the importance of a 3'-hydroxyl group on the cytotoxic properties (Table 5). Moreover, combrestatin A4-like **24** exhibits interesting activity against tubulin polymerization (IC<sub>50</sub> = 16.3 μM), binds colchicine site (IC<sub>50</sub> = 36 μM) and results in a significant cell cycle arrest at the G2/M point (73.4 *vs.* 27.5 for the control). These encouraging results demonstrate that the Z-double bond spacer present in combrestatin A4 could be carefully replaced by another spacer-like ether link. Further SAR studies would be needed to

**Table 5** Cell growth inhibition and effects upon tubulin binding

Compounds	IC <sub>50</sub> <sup>a</sup> (μM)	IC <sub>50</sub> <sup>b</sup> (μM)	IC <sub>50</sub> <sup>c</sup> (μM)
	K562 cell line	Tubulin assembly	Colchicine displacement
<b>24</b>	0.05	16.3	36
<b>25</b>	0.38	—	—
Combrestatin A4	0.0026 (P388 murine cell line)	0.5 to 2	—

<sup>a</sup> K562 Cell growth inhibition measured by the MTT assay after 5 days incubation of the drug with the cells cultured at 37 °C. <sup>b</sup> The IC<sub>50</sub> values represent the concentrations for a 50% decrease in tubulin assembly as measured by an increase in turbidity at 350 nm. <sup>c</sup> The IC<sub>50</sub> values represent the concentrations for a 50% decrease in the binding of <sup>3</sup>H-colchicine from purified porcine tubulin.

**Scheme 4** Synthesis of diaryl ether combrestatin A-4 analogs.



**Scheme 5** Synthesis of methylene imidazole diaryl ethers.

transform diaryl ether combrestatin A4-like in a lead for anti-cancer research.

**2.4.2. Other acyclic non-natural diaryl ethers.** Herein we report the synthesis of diaryl ethers with very different biological targets to illustrate an interesting multitude of routes explored to discover an anti-cancer agent.

Ras proteins are G proteins playing pivotal roles in the control of normal and transformed cell growth. Mutated forms of ras-protein found in many human tumors are unable to regulate themselves and hence remain constantly activated, leading to uncontrolled cell growth.<sup>48</sup> A farnesylation on C-terminal by a farnesyl-protein transferase (FPTase) is required to induce malignant transformation. Many investigations were prompted to design farnesyl transferase inhibitors (FTIs) as novel anti-cancer drugs.<sup>49</sup> In this aim, S. MacTough and co-workers<sup>50</sup> prepared a series of diaryl ethers as potent inhibitors of FTPase. 4-Bromo-3-fluorotoluene (**26**) was oxidized to the corresponding benzoic acid by using  $\text{KMnO}_4$  in water in the presence of pyridine (Scheme 5). The subsequent carboxylic acid was reduced to alcohol by  $\text{BH}_3$  in THF. Palladium catalyzed cyanation of aryl bromide followed by a radical bromination gave the 4-(bromomethyl)-2-fluorobenzonitrile (**27**). Imidazole was introduced by nucleophilic substitution. Diaryl ethers **28** and **30** were synthesized by aromatic nucleophilic substitution with different commercially available phenols in DMF.

We focused here on the most active diaryl ethers as FPTase inhibitors (Table 6). The structure–activity relationship showed that single chlorine substitution on the aryl part increased FPTase inhibition activity (4-fold). Phenyl substitution in the

*meta*-position with a methoxy group increased inhibition.<sup>50</sup> Double methoxy (**28c**) or Cl-halogen (**28b**) substitution led to the best activities against FPTase with  $\text{IC}_{50} = 1 \text{ nM}$  and  $8 \text{ nM}$  respectively. Moreover a great selectivity between FPTase and GGTase-I inhibition was observed.

However, it has been found that when treated with FTIs, mutated forms of Ras proteins are alternatively prenylated by geranylgeranyl transferase-I (GGPTase-I). To avoid this behavior, the same team developed a new family of inhibitors based on the chemical structure of compound **36** with dual inhibition properties against FPTase and GGPTase-I (Table 7).<sup>51</sup>

In the first part, a Parikh–Doering oxidation of alcohol **31**, followed by a Grignard addition on the corresponding aldehyde led to the subsequent secondary alcohol which was converted ultimately to acetate **32** under usual conditions. Nitrogen imidazole was then methylated using dimethylsulphate. The trityl group was removed by methanolysis and acetate was hydrolyzed to give the corresponding alcohol **33** which was converted to amine **34** by sequential treatment with thionyl chloride and ammonia. In the second part, enolate derived from amide **36** was reacted with methoxybenzyl derived from precursor **35**. Subsequent alkylation by using iodoethane under basic conditions followed by demethylation with boron tribromide gave phenol **29**. Before demethylation, a chiral-phase chromatography resolution can be realized to obtain the optically pure enantiomers. Arylation of phenol **29** using KF/alumina occurred in the presence of fluoroaryl **40** to provide the corresponding diaryl ether. Methylation and methanolysis steps led to the azepinone diaryl ether **37**. Compound **38** was synthesized using the same coupling procedure starting from (+/–)**33**, followed by sequential use of thionyl

**Table 6** Inhibition of prenylation activity

Compounds	Ar	FPTase $\text{IC}_{50}$ (nM)	GGPTase-I $\text{IC}_{50}$ (nM)
<b>28a</b>	Ph	230	$3700 \pm 900$
<b>28b</b>	2,4-DiCl-Ph	8	280
<b>28c</b>	2,3-DiOCH <sub>3</sub> -Ph	1	15 000
(+/-)- <b>30</b>		2.9	7.1

**Table 7** Inhibition of prenylation activity of azepinone diaryl ethers (mixture of diastereoisomers or optically pure)

Compounds	FPTase $\text{IC}_{50}$ (nM)	GGPTase-I $\text{IC}_{50}$ (nM)
(S) <b>30</b>	1.4	5.8
(+/-)- <b>37</b>	0.6	10
<b>38</b>	0.19	8
<b>39</b>	0.38	5.1
(S,S)- <b>39</b>	0.06	3.6

chloride and ammonia. Arylation conditions used in the presence of **29** and (+/–)**34** gave a benzylic amine which underwent autooxidation to give an intermediate ketone. The latter was treated with bromomethyl magnesium to introduce a methyl group on the benzyl position before the conversion of alcohol into amine to give compound **39** (Scheme 6).

Resolution of the racemic compound **30** revealed that the *S* enantiomer is the most potent inhibitor of both FTase and GGTase-I *in vitro* (FTase IC<sub>50</sub> = 1.4 nM, GGTase-I IC<sub>50</sub> = 5.8 nM) (Table 7). The structure–activity relationship studies showed some interesting points. The presence of an ethyl group was important to ensure the potent inhibition activity. The change of the substitution position on the imidazole part from N-1 (**30**) to C-5 (**37–39**) induced less potent activity which was avoided by adding a methyl substitution on N-1 (data not shown).<sup>51</sup> Because of the encouraging activity of azeponone diaryl ether **38**, a methyl substituent was added on the benzylic position in derivatives of **39** in order to increase metabolic stability. The four diastereoisomers of **39** were prepared starting from the appropriate enantiomers of phenol **29** and fluorophenyl **34**. Only the (*S,S*)-**39** revealed more potent inhibition on FPTase than the mixture of four isomers **39**. This result was supported by a crystal structure of human farnesyltransferase obtained with compound (*S,S*)-**39** bound to the active site. The crystallographic data suggested a competitive mechanism of inhibition as a protein substrate.<sup>52</sup> *In vivo* evaluation in nude mice bearing PSN-1 tumor xenografts treated for 72 h with doses of inhibitors sufficient to inhibit K-Ras processing demonstrated the anti-tumor efficacy of agent (*S,S*)-**39** complicated by severe toxicity.<sup>53</sup> These results may limit the therapeutic benefit of (*S,S*)-**39** as an anti-cancer dual drug.

Matrix metalloproteinases (MMPs), zinc dependent endopeptidases, have been regarded as major critical molecules assisting tumor cells during metastasis. There has been a clear connection between MMPs, extracellular matrix degradation and cancer cell invasion. Numerous studies linked the inhibition of MMPs by synthetic and natural inhibitors (tissue inhibitors of matrix metalloproteinase, or TIMPs) with a corresponding inhibition of cell invasion.<sup>54</sup> In this context, C. K Wada and co-workers (2002) discovered a family of phenoxyphenyl sulphone *N*-formylhydroxylamines inhibiting MMP-2 and 9 closely associated with tumor progression.<sup>55</sup> Based on a previous work,<sup>56</sup> SAR studies led them to improve the MMP-2 and 9 inhibitions over MMP-1 of **ABT-770** by replacing it with **ABT-518**. Insertion of diaryl ether linkage induced selectivity and anti-tumor activity improvements (Fig. 5).

To identify **ABT-518** as a good clinical candidate, a different family of compounds with various modifications were prepared

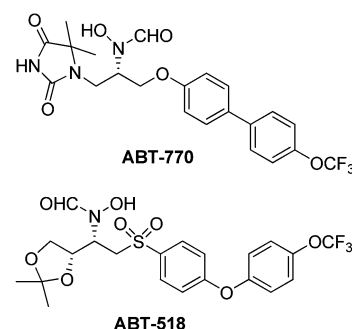
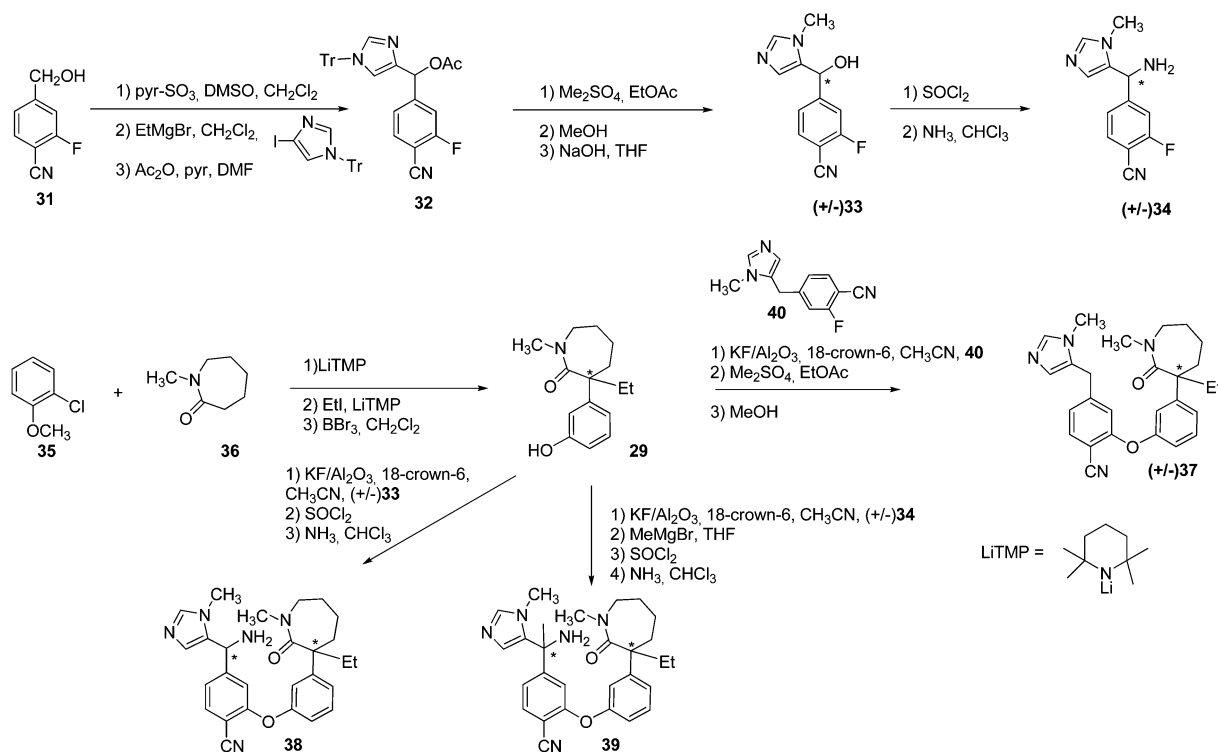
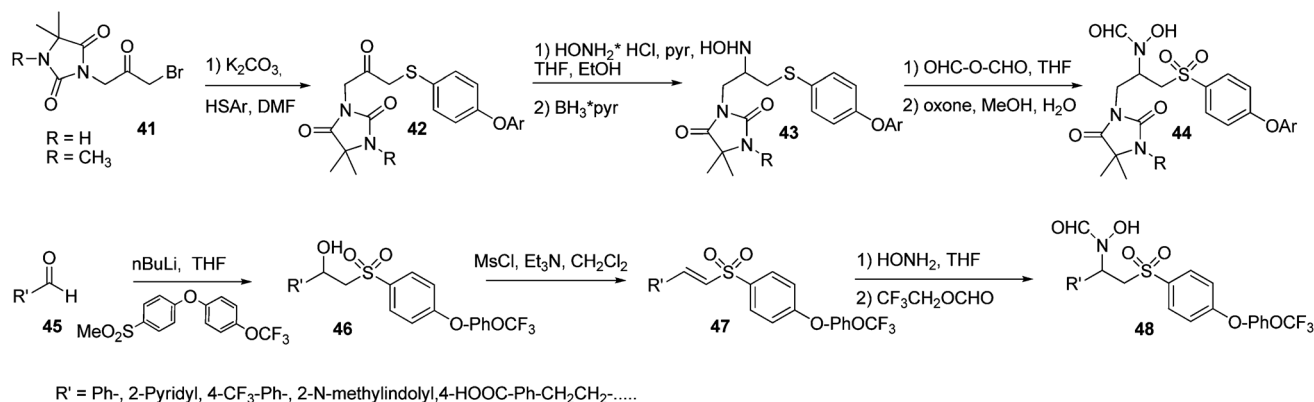


Fig. 5 Ether and sulphone retrohydroxamates.



Scheme 6 Preparation of the most active azeponone diaryl ethers.



**Scheme 7** Hydantoin sulphone retrohydroxamates **44** and aryl sulphone retrohydroxamates **48** synthesis.

and investigated. Herein, the most effective derivatives of each family are presented.

*R*-Substituted bromomethylketone **41** reacted rapidly with the arylthiol in the presence of  $\text{K}_2\text{CO}_3$  in dimethylformamide (DMF) at  $-5^\circ\text{C}$  (75–90% yield). A three-step sequence was used to install the retrohydroxamate group (50–80% overall yield). Ketone molecules of **42** were converted to the corresponding oxime by treatment with hydroxylamine hydrochloride in the presence of pyridine. This oxime was then reduced to the hydroxylamine using complex borane\*pyridine/4 N HCl-dioxane. Formylation of the hydroxylamine **43** was carried out with acetic formic anhydride at  $0^\circ\text{C}$  in tetrahydrofuran. Finally, the sulphide oxidation to the sulphone **44** was carried out by treatment with oxone in methanol/ $\text{H}_2\text{O}$  (Scheme 7).

In order to prepare the derivative **48**, the lithium anion of the aryl methyl sulphone was formed by treatment with *n*-butyllithium at  $-78^\circ\text{C}$  in THF to which was added the aldehyde **45** at  $-78^\circ\text{C}$  affording the corresponding alcohol **46**.  $\alpha$ -Hydroxy-sulphone **46** was first converted to the  $\alpha,\beta$ -unsaturated sulphone **47** by formation of the mesylate followed by elimination. Treatment of the  $\alpha,\beta$ -unsaturated sulphone **47** with aqueous hydroxylamine in THF led to the 1,4-Michael adduct in a good yield. *N*-Formylation by using trifluoroethyl formate<sup>57</sup> in refluxing THF or MTBE gave the desired *N*-formyl product **48**.

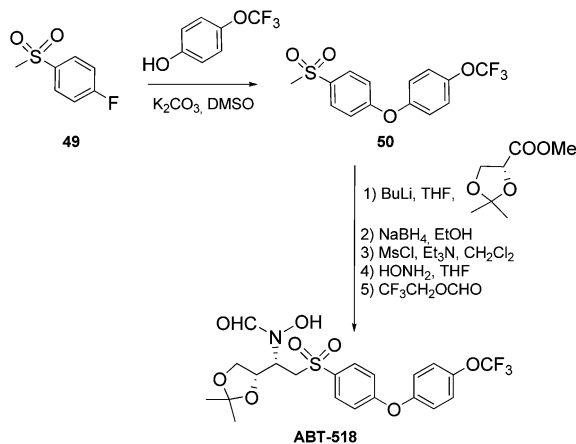
Biaryl methyl sulphone **50** was prepared by a nucleophilic aromatic substitution of 4-fluoro-1-methylsulfonylbenzene by 4-

trifluoromethoxyphenol under basic conditions in DMSO at  $120^\circ\text{C}$ . Methyl sulphone **50** was treated with *n*-butyllithium and added to (*R*)-methyl 2,2-dimethyl-1,3-dioxolane-4-carboxylate at  $-78^\circ\text{C}$  in THF to give the corresponding ketone in 79% yield (>99% ee). The ketone was then reduced with sodium borohydride to the corresponding alcohol. **ABT-518** was obtained by following the same procedure as described in Scheme 7. Analysis of the final product by chiral high performance liquid chromatography (HPLC) established the enantiomeric excess of **ABT-518** as >99% (Scheme 8).

In the hydantoin sulphone retrohydroxamates **44**, the presence of a methyl group on N-1 position ( $R = \text{Me}$ ) and of a trifluoromethyl substituent on the aryl (Ar) part increased selectivity (until 27 000-fold) between MMP-1 and MMP-2/MMP-9. It is noteworthy that biaryl ether moiety does not affect selectivity compared to biaryl derivatives. Moreover, the observed poor bioavailability could be explained by weak solubility.

In the further exploration of structure–activity relationships to improve oral exposure, aryl sulphone retrohydroxamates **48** with different substituents (*R* group, Scheme 7) have been synthesized and tested against MMP-1, -2 and -9. Some of the most interesting results are presented in Table 8.

Introduction of carboxylic acid (**48a**) induced a high potent (<1 nM) and selective (>10 000-fold) MMP inhibitor. Acyclic sulphone retrohydroxamates with an ether side chain (**48b**) and heterocyclic sulphone retrohydroxamates presented the most selective capacity for the inhibition of MMP-2 and -9 over MMP-1 with no activity against MMP-1 (>50  $\mu\text{M}$ ). For each inhibitor, no improvement in the pharmacokinetic properties was observed. Diaryl ether retrohydroxamate **ABT-518** was the most promising inhibitor, with excellent selectivity (>11 400-fold), strong inhibition activity ( $\text{IC}_{50} = 0.5 \text{ nM}$  against MMP-9) and good bioavailability ( $\text{AUC} = 53 \mu\text{M h}$ ). Slight modifications on the acetonide part induce a decrease of inhibition activity (**48f-g**). **ABT-518** demonstrated anti-tumor activity when administered orally (twice a day over a period of 7–21 days) as a monotherapy in a murine syngenic tumor growth model (48% inhibition of tumor growth to 2 g relative to control at 30 mpk). **ABT-518** was undergone on phase I clinical trials in cancer patients. Radio labeled **ABT-518** was prepared in seven steps in 2009 to study its ADME properties<sup>58</sup> even if no more information is available to date in the literature on this study.



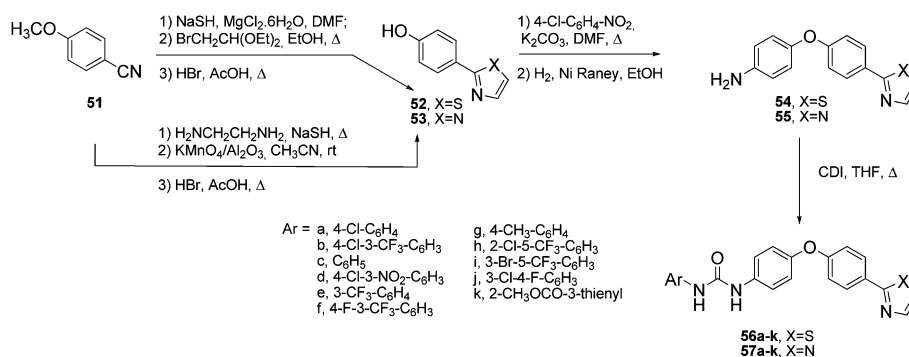
**Scheme 8** Preparation of **ABT-518**.



**Table 8** Aryl, acyclic and heterocyclic sulphone retrohydroxamates inhibition activity (IC<sub>50</sub>), half time of life (*t*<sub>1/2</sub>) and bioavailability (AUC)

compound	R	IC <sub>50</sub> (nM)			<i>t</i> <sub>1/2</sub> (iv)/AUC (po) <sup>a</sup>
		MMP-1	MMP-2	MMP-9	
<b>48a</b>		>50 000	0.53	0.53	nd/16 μM h
<b>48b</b>		>50 000	0.44	0.30	1.91 h nd <sup>-1</sup>
<b>48c</b>		>50 000	0.61	0.32	nd/26 μM h
<b>48d</b>		>50 000	0.36	0.092	1 h/3 μM h
<b>48e</b>		>50 000	0.42	2.0	nd/28 μM h
<b>ABT-518</b>		8900 ± 4700 (2)	0.78 ± 0.2 (2)	0.50	16.8 h/53 μM h
<b>48f</b>		>50 000	1.9	1.1	19.5 h/21 μM h
<b>48g</b>		>50 000	1.5	5.5	nd/2 μM h

<sup>a</sup> Three mpk in cynomolgous monkey; *n* = 1 (iv); *n* = 2 po.

**Scheme 9** Synthetic route for the preparation of diaryl ether urea series.

Sorafenib, a diaryl urea, is an approved anti-cancer drug used in USA since 2005, acting as inhibitor of several kinases implicated in tumor proliferation and angiogenesis.<sup>59</sup> Based on sorafenib as a lead, M. Sun and co-workers (2010) prepared two series of diaryl ether urea and evaluated their cytotoxic profiles (Scheme 9).<sup>60</sup>

4-Methoxybenzonitrile **51** was used as starting material for the synthesis of the two series. Thioamide **52** was synthesized in three steps: addition of sodium hydrogen sulphide in the presence of magnesium chloride on the nitrile **51** led to the corresponding benzothiamide which was treated with bromoacetaldehyde diethyl acetal to yield the corresponding thioamide. Demethylation was prepared under strong acidic conditions to give the expected compound **52**. The imidazole ring was obtained *via* a dehydrogenation of the corresponding imidazoline obtained from benzonitrile **51**. Further nucleophilic substitution of 4-chloronitrobenzene by the phenate of the compounds **52** or **53**

followed by a reduction of the nitro group gave the corresponding diaryl ethers **54** and **55**. Diaryl ureas (**56a-k**, **57a-k**) were obtained by a coupling reaction with different arylamines using *N,N'*-carbonyldiimidazole.

Cytotoxicity of the agents was investigated on A549 (human lung adenocarcinoma epithelial cells) and MDA-MB-231 (human breast cancer cell) cell lines *in vitro*; most active compounds are presented in Table 9.

The cytotoxic activity screening (data not shown here) indicates that the compounds **56** attached to a thiazole ring are more potent than compounds **57** with an imidazole moiety. The authors suggested that the higher hydrophobicity of series **57** could explain the lower cytotoxicity<sup>60</sup> because of their poor membrane permeability. Moreover, Table 9 reveals that the cytotoxic activity should be related to the electronic effect on the aromatic ring connected to the urea group. A strong electron-withdrawing substituent such as nitro (**56d**) or trifluoromethyl

**Table 9** Cytotoxic activity (IC<sub>50</sub>) of target diaryl ether urea against A549 and MDA-MB-231 cell lines

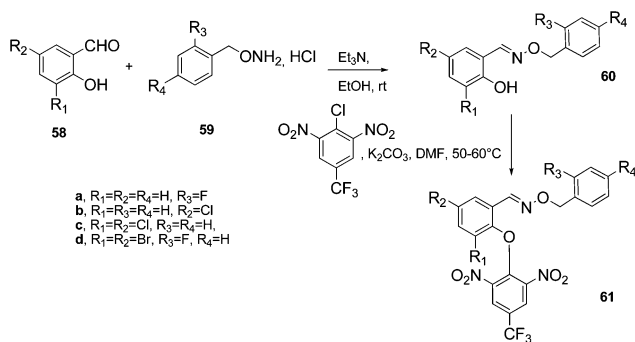
Compounds	A549 <sup>b</sup> IC <sub>50</sub> (μM)	MDA-MB-231 <sup>b</sup> IC <sub>50</sub> (μM)
<b>56b</b>	3.81	6.06
<b>56d</b>	3.89	6.87
<b>56f</b>	4.98	8.66
<b>56i</b>	2.71	4.19
<b>57b</b>	7.09	NT <sup>a</sup>
<b>57f</b>	10.52	NT <sup>a</sup>
Sorafenib	5.21	7.62

<sup>a</sup> NT: no test. <sup>b</sup> IC<sub>50</sub> is the concentration of compound required to inhibit the cell growth by 50% compared to an untreated control.

(**56e**) induced high cytotoxicities. Moreover, the halogen substitution in the presence of strong electron-withdrawing substituent groups on the *meta*-position of a benzene ring has been found to improve cytotoxicities to various extents. Generally, chemical agents with a *para*-chloro substitution gave better activity than those with fluoro and *ortho*-chloro substitution. Furthermore, compounds with *meta*-bromo substitution demonstrated the strongest cytotoxic activities. Compared to contrast drug sorafenib, **56b**, **56d**, **56f** and **56i** were found to be more potent anti-tumor agents.

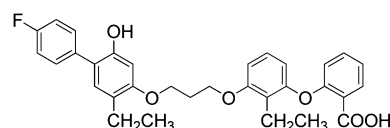
The oxime frame displays anti-cancer<sup>61,62</sup> properties due to the exocyclic –RC=N– bond. T.-T. Zhao and co-workers<sup>63</sup> (2012) designed new salicylaldoximes, expecting that the introduction of the 1,3-dinitro-5-(trifluoromethyl)phenoxy group could contribute to the binding of target compounds with tubulin. Synthesis of the most potent diaryl ethers, salicylaldoximes, is reported in Scheme 10. Different substituted *O*-benzylhydroxylamines hydrochloride **59** reacted with substituted salicylaldehydes **58** in the presence of triethylamine to generate salicyloxime derivatives **60**. Then the further coupling reaction with 2-chloro-1,3-dinitro-5-(trifluoromethyl)benzene in the presence of potassium carbonate led to the corresponding diaryl ethers salicylaldoximes **61**.

All the synthesized compounds were tested for the anti-proliferative activities against three different tumor cell lines MCF-7, Hep-G2 (human hepatocellular liver carcinoma cell) and A-549 and for their ability to inhibit tubulin polymerization (see Table 10). When compared to colchicine or combrestatin A4, diaryl ether salicylaldoxime **61a** presented the best anti-proliferative and tubulin polymerization inhibition properties

**Scheme 10** General synthesis of the most potent diaryl ethers, salicylaldoximes.**Table 10** Inhibition (IC<sub>50</sub>) of MCF-7, Hep-G2 and A549 cells proliferation and inhibition of tubulin polymerization<sup>c</sup>

Compounds	IC <sub>50</sub> ± SD (μM)			
	MCF-7 <sup>a</sup>	Hep-G2 <sup>a</sup>	A549 <sup>a</sup>	Tubulin <sup>b</sup>
<b>61a</b>	0.70 ± 0.05	0.68 ± 0.02	0.86 ± 0.05	3.06 ± 0.05
<b>61b</b>	1.22 ± 0.13	1.79 ± 0.07	3.41 ± 0.28	30.89 ± 2.16
<b>61c</b>	0.80 ± 0.09	0.82 ± 0.18	1.23 ± 0.02	3.65 ± 0.18
<b>61d</b>	0.88 ± 0.07	1.10 ± 0.08	1.56 ± 0.05	4.53 ± 0.08
CA-4	0.41 ± 0.04	0.19 ± 0.04	0.09 ± 0.01	0.70 ± 0.20
Colchicine	0.53 ± 0.07	0.23 ± 0.02	0.75 ± 0.08	1.72 ± 0.18

<sup>a</sup> Tumor cell lines growth inhibition. <sup>b</sup> Tubulin polymerization inhibition. <sup>c</sup> CA-4: combrestatin A4, SD: standard deviation.

**Fig. 6** Chemical structure of LY293111 (LY).

indicating that the anti-proliferative effect was produced by a direct connection between tubulin and compound **61a**.<sup>63</sup>

Further experiments by flow cytometry showed that derivative **61a** could induce the apoptosis of activated MCF-7 cells in a dose-dependent manner. The molecular docking (LigandFit Dock protocol of Discovery Studio 3.1) performed by simulation of compound **61a** into the colchicine binding site of tubulin (PDB code: 1SA0) showed that the **61a** derivative well embedded in the active pocket with three hydrogen bonds. All these results have indicated that compound **61a** might be a strong tubulin polymerization inhibitor.

LY293111 (LY) (Fig. 6), a novel diaryl ether carboxylic acid derivative, is a novel oral anti-cancer agent with leukotriene B<sub>4</sub> receptor antagonist and peroxisome proliferator-activated receptor gamma agonist properties, producing promising results alone and in combination with gemcitabine in pancreatic cancer xenograft models. In 2005, a phase I study proved that the combination (gemcitabine plus LY) was a safe and well-tolerated drug.<sup>64</sup>

Unfortunately in 2009, a randomized double-blind phase II trial comparing gemcitabine plus LY293111 *versus* gemcitabine plus placebo in advanced adenocarcinoma of the pancreas did not demonstrate any benefit to adding LY to gemcitabine in untreated patients with advanced pancreatic carcinoma.<sup>65</sup>

### 3. Natural and non-natural macrocyclic diaryl ethers

#### 3.1. Macrocyclic diaryl heptanoid

Macrocyclic diaryl ether heptanoid (MDEH) forms a subgroup of the diarylheptanoid family of natural products. Compounds of this class exhibit a wide range of biological activities including anti-cancer, anti-inflammatory, anti-fungal, and anti-bacterial effects.<sup>66</sup> The common structural core is a diaryl ether moiety connected by seven carbon atoms. (*R*)-Platycaryanol, a natural MDEH, was shown to inhibit a nuclear factor of κB (NF-κB), a sequence-specific transcription factor known to be involved in the

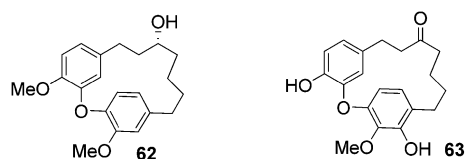


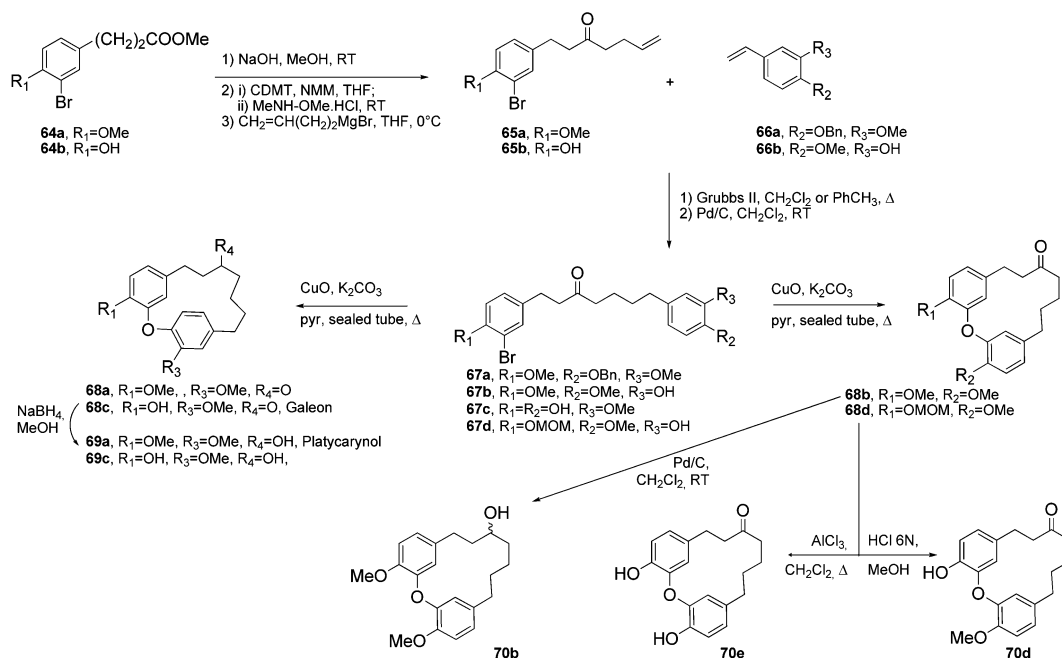
**Fig. 7** Chemical structures of diaryl ether heptanoids isolated from *Alnus hirsuta*.

inflammatory and innate immune responses. Recent evidence indicates that NF- $\kappa$ B and the signalling pathways that are involved in its activation are also important for tumour development,<sup>67</sup> particularly in pancreatic cancer.<sup>68</sup> Among diaryl ether heptanoids isolated from *Alnus hirsuta*, macrocycles **62** and **63** (Fig. 7) exhibited a potent NF- $\kappa$ B mediated reporter gene expression inhibition with  $IC_{50}$  values 9.2 and 9.4  $\mu$ M, respectively (partenolide ( $IC_{50}$  = 3.4  $\mu$ M) was used as a positive control).<sup>69</sup>

Based on this information, Bryant and co-workers<sup>70</sup> (2012) synthesized native platycaryinol and galeon and some analogs by using Ullmann coupling and olefin metathesis reaction as chemical strategic steps.

Esters **64a** and **b** were saponified. The corresponding acids were converted to the Weinreb amide which reacted under Grignard conditions with 3-butenylbromide to give keto-alkenes **65a** and **b**. Metathesis coupling with styrenes **66a** and **b** using the Grubbs II catalyst followed by double bond hydrogenation gave biaryl ketones **67** in moderate yield (Scheme 11). On one hand, macrocyclization of fragments **67a** and **c** using copper oxide in a sealed tube resulted in a *meta-para* linked MDEH analog **68a** and the natural diaryl ether, galeon **68c**. Reduction of the ketone in **68a,c** resulted in racemic platycaryinol **69a** and analog **69c**. On the other hand Ullmann cyclization of fragments **67b** and **67d** resulted in a *meta-meta* linked MDEH analogs **68b** and **d**. Analog **70b** was obtained by reduction of the ketone in **68b**. Removal of the MOM protecting group in **68d** yielded a monomethylated analog **70d** while treating **68b** with aluminium chloride led to the analog **70e**.

This small library of MDEH analogs were screened as NF- $\kappa$ B inhibitors in stable  $\kappa$ B-luciferase expressing A549 cells at 20  $\mu$ M. Compound **68b** ( $IC_{50}$  = 14.3  $\mu$ M) and platycaryinol ( $IC_{50}$  = 36.4  $\mu$ M), the most active *meta-meta* and *meta-para* diaryl ether compounds, exhibited the best NF- $\kappa$ B inhibition activities which



**Scheme 11** Synthesis of MDEHs.

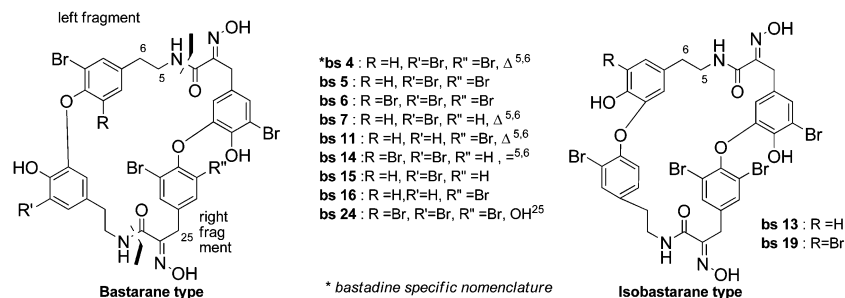


**Fig. 8** Some bastadins (bs) structures.

were ~3 fold less than the parthenolide one ( $IC_{50} = 4.7 \mu M$ ), a known NF- $\kappa B$  inhibitor. Further experiments have shown **68b** sensitized Hs 766T and PANC-1 cells to chemotherapeutic agent gemcitabine mediated growth inhibition and **68b** sensitized PANC-1 cells to gemcitabine mediated caspase activation. These results should suggest using **68b** as adjuvant and not as chemotherapeutic agent hit.

### 3.2. Bastadin

Marine organisms are well known to contain an important variety of potent anti-cancer substances. Some of them, bastadins isolated from different marine sponges (*Ianthella basta*, *Ianthella quadrangulata* or *Dendrilla cactos*), show a typical organic skeleton: a bis-macrocyclic diaryl ether formed by assembling two fragments (left and right) consisting of altered dopamine and highly brominated tyrosines.<sup>71</sup> The bastadin family is divided into two categories: bastaranes and isobastaranes types. The difference is based on the biphenyl ether linkage of the left half of the fragment: *meta-para* for the bastarane family and *para-meta* for the isobastarane molecules (Fig. 8).

The presence of two amide bonds and two diaryl ether links endows to this molecule a “good” stability against chemical degradation. The different types of bastadins depend on the degree of bromination, their position and the presence or absence of a double bond ( $C_5-C_6$ ).

Bastadin alkaloids exhibit a wide variety of biological activities. In 2006, A.V. Reddy *et al.*<sup>72</sup> demonstrated an anti-cancer activity by different bastadins against Sup-T1 cancer cells (T cells lymphoma) (Table 11).

Bastadins **bs6** and **bs16** are the most efficient with  $IC_{50}$  values in the subnanomolar range demonstrating the potentiality of these natural alkaloids for anti-cancer research area.

At the same time, bastadin **bs24**, the 25-hydroxy derivative of bastadin **bs6** newly isolated from the Australian sponge *Ianthella quadrangulata*, among the 36 investigated by H Greve *et al.*<sup>73</sup> exhibited selective cytotoxicity toward 5 human tumor cell lines (CNXF SF268 (glioblastoma,  $IC_{50} = 0.38 \mu g mL^{-1}$ ), LXFA 629L (lung adenocarcinoma,  $IC_{50} = 0.37 \mu g mL^{-1}$ ), MAXF 401NL (mammary cancer,  $IC_{50} = 0.55 \mu g mL^{-1}$ ), MEXF 276L (melanoma,  $IC_{50} = 0.59 \mu g mL^{-1}$ ), and PRXF 22RV1 (prostate cancer,  $IC_{50} = 0.46 \mu g mL^{-1}$ )).

As before, **bs6** showed the lowest  $IC_{50}$  value while **bs24** combined concentration-dependent inhibition of tumor cell proliferation and significant tumor cell selectivity (Table 12). Moreover, this cytotoxic selectivity pattern did not act according to the known mechanism of action of standard cytotoxic agents, giving interest to **bs24** as new hit.

**Table 11** *In vitro* cytotoxic activity of bastadins on Sup-T1 cells

Compound	$IC_{50}$ (nM) on Sup-T1 cells
<b>bs6</b>	0.079
<b>bs12</b>	8
<b>bs14</b>	140
<b>bs15</b>	645
<b>bs16</b>	0.001
<b>bs19</b>	73

**Table 12** Mean *in vitro* cytotoxic activity of bastadins on different tumor cell lines

Compound	Mean $IC_{50}$ ( $\mu g mL^{-1}$ ) <sup>a</sup>
<b>bs24</b>	1.8
<b>bs4</b>	2.9
<b>bs5</b>	2.2
<b>bs6</b>	0.7
<b>bs7</b>	3.2
<b>bs13</b>	2.4

<sup>a</sup> Mean  $IC_{50}$  values resulting from 36 different human tumor cell lines comprising 14 solid tumor types.

In order to explore the way of cytotoxicity, bastadins were evaluated as anti-angiogenic agents on human umbilical vein endothelial cells (HUVEC) to support their anti-cancer potentiality. Only **bs7** and **bs12** inhibited the serum + hEGF induced (human epithelial growth factor) tubular formation of HUVEC cells at  $1 \mu g mL^{-1}$  concentration compared to the control experiments (37.3% and 27.6% inhibition, respectively).

These bastadins angiogenesis inhibition properties were also explored by Kotoku and co-workers<sup>74</sup> (2005).

Only bastarane type derivatives exhibited potent anti-proliferative activities against HUVECs under bFGF-dependent conditions with a 38- to 76-fold selectivity as shown in Table 13. No selective anti-proliferative activities were observed, when tested on other cell lines (Neuro2A, K562 and 3Y1) as doxorubicin and etoposide used as chemotherapeutic drugs. In order to elucidate the impact of bastarane or isobastarane skeleton on the anti-proliferative activity, global conformational analyses were carried out by using Monte Carlo Multiple Algorithm (MCMC). This molecular mechanics calculation demonstrated that rigid conformation of the bastarane skeleton was an important structural factor for all derivatives of this family.

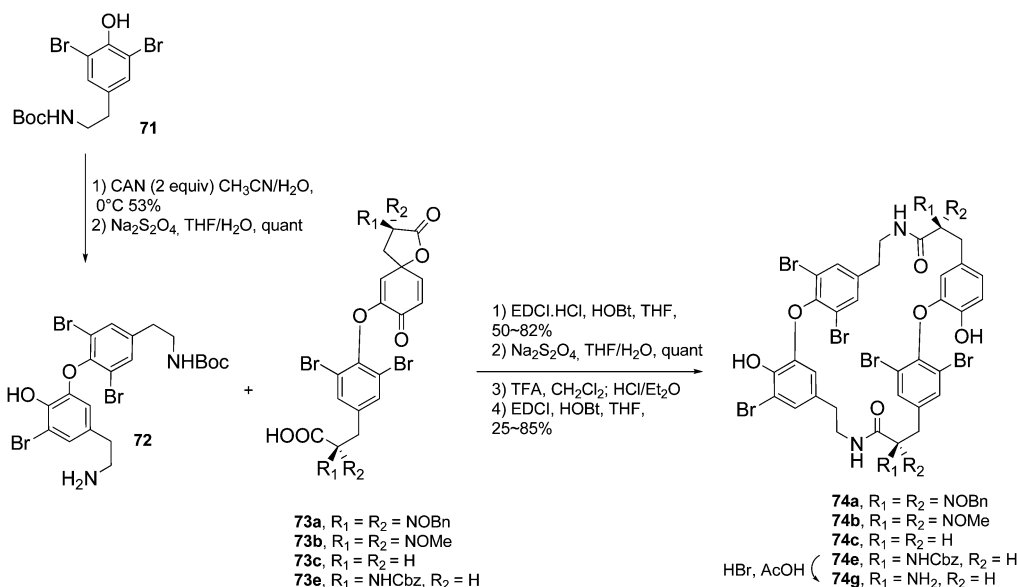
Based on these first results, the same authors synthesized bastadin **bs6** analogs by the modulation on the bromine atoms number and oxime functionality in such a way as to enable the structure–activity relationships.

Diaryl ethers were synthesized through an oxidative coupling of the 2,6-dibromophenol derivative **71** mediated by CAN (cerium ammonium nitrate) followed by a subsequent reductive aromatization with  $Na_2S_2O_4$ .<sup>75</sup> Left and right fragments were assembled by using EDCI·HCl as a coupling agent (Scheme 12).

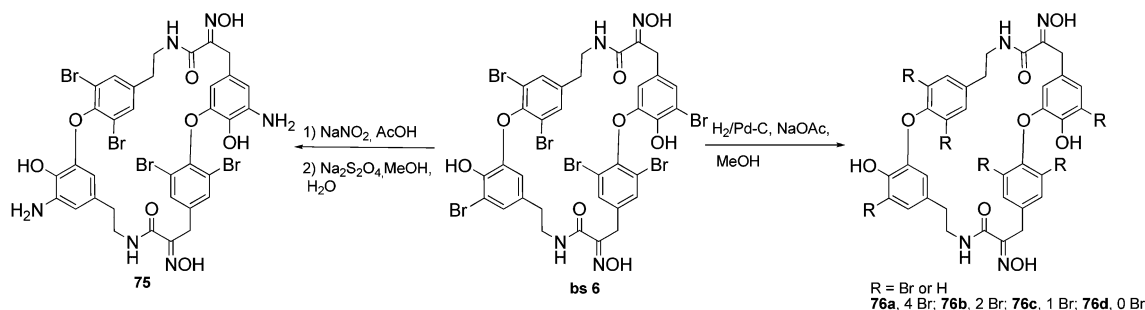
**Table 13** *In vitro* anti-proliferative activity of bastadins and selective index

Compound	$IC_{50}$ ( $\mu M$ ) <sup>a</sup>	SI <sup>b</sup>
<b>bs4</b>	0.053	38
<b>bs5</b>	0.062	76
<b>bs6</b>	0.052	41
<b>bs7</b>	0.054	56
<b>bs11</b>	0.053	38
<b>bs13</b>	0.52	14
<b>bs19</b>	0.12	19

<sup>a</sup>  $IC_{50}$ , The concentration required for 50% inhibition of proliferative activity of HUVEC cultured in the medium containing only basic fibroblast growth factor (bFGF) as a growth factor. <sup>b</sup> SI selective index:  $IC_{50}$  against testing KB3-1cells/ $IC_{50}$  against HUVEC (bFGF-dependent conditions).



Scheme 12 Synthesis of bromine-modified bastadine analogs.



Scheme 13 Synthesis of oxime-modified bastadine bs6.

Under hydrogenolysis conditions (Scheme 13), **bs6** gave a mixture of partially debrominated derivatives isolated in a pure form after HPLC separation. The bromine position in **76a–c** analogs was not clearly assigned because of ambiguous NMR spectra. In order to increase solubility of **bs6**, two bromine atoms were selectively substituted by nitro groups which were subsequently reduced to give diamino analog **75**.

Anti-proliferative activities against HUVEC cells were evaluated and the best among them are presented in Table 14.

First of all, the chemical modifications on oxime functionality and the number of bromine atoms present have been observed to decrease the growth inhibitory activity in relation to **bs6**. Nevertheless, oxime is found to be important for the anti-proliferative activity. When the oxime functionality is missing (**74c**), a loss of activity and selectivity is noted. Moreover, more than two bromine atoms (**76a** and **b**) are needed to retain anti-proliferative effects and a good selective index. Molecular mechanics calculations confirm that the presence of bromine atoms is related to the preservation of the rigid conformation of bastadine. NH<sub>2</sub>-analog **75** also exhibits strong macrocyclic rigidity even if the anti-angiogenic activity is 18-fold higher than that of **bs6** indicating that conformational properties are not the only factor influencing the biological activity.

### 3.3. Macrocyclic bisbibenzylethers

Macrocyclic bisbibenzyls (*e.g.* marchantins, riccardins and plagiocins) are characteristic constituents of liverwort species.<sup>76</sup> In these molecules, two substituted bisbibenzyls are joined by two diaryl ether bonds or one diaryl ether and one biphenyl bond each (Fig. 9). Marchantins, the largest family group of the first class, exhibit anti-bacterial, anti-fungal and cytotoxic activities. This paragraph focuses on the latter property.

**Table 14** *In vitro* growth inhibitory activity and selective index of bastadin analogs

Bastadine-analogs	IC <sub>50</sub> (μM) HUVEC	SI <sup>a</sup>
<b>bs6</b>	0.052	41
<b>74c</b>	4.0	1.6
<b>74g</b>	0.61	26.2
<b>76a</b>	0.16	27
<b>76b</b>	0.48	35
<b>75</b>	0.96	3.4

<sup>a</sup> SI selective index: IC<sub>50</sub> against testing KB3-1cells/IC<sub>50</sub> against HUVEC cells.



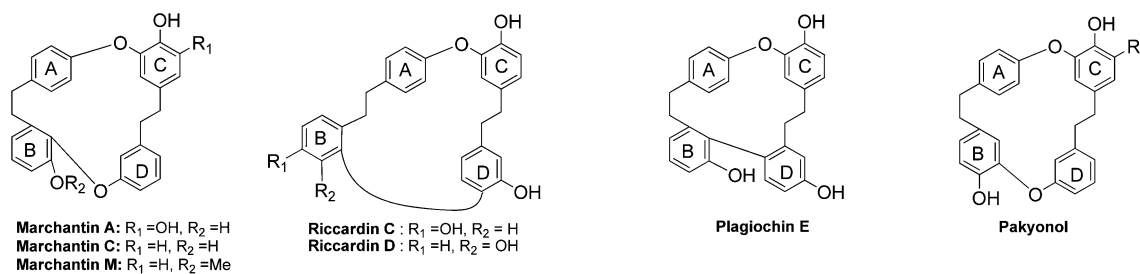


Fig. 9 Examples of natural bisbibenzyl chemical structures.

Success in cancer chemotherapy is challenged by the development of tumors having a multi-drug resistance (MDR) phenotype. It is one of the major causes of the failure of cancer chemotherapy. MDR is a multi-factorial problem, where several mechanisms act in concert with each other for the development of the MDR phenomenon. One of the most recognized is related to the frequent overexpression of ATP-binding cassette (ABC) transporters on the plasma membrane of cancer cells, such as P-glycoprotein (P-gp).<sup>77</sup> P-gp, a 170 kDa transmembrane protein, is encoded by the MDR1 gene. The latter is now the best characterized drug transporter. It can actively efflux a wide range of structurally and functionally related or unrelated anti-cancer drugs out of cancer cells. This consequently decreases their intracellular levels to a sublethal concentration and reduces their therapeutic efficacy.<sup>78</sup> Lou and co-workers<sup>79a</sup> (2009) focused their research on natural macrocyclic bisbibenzyls as potent multidrug resistance inhibitors and more specifically P-glycoprotein one. K562/A02 cells, a multidrug-resistant chronic myeloid leukemia cell line, were used in their studies. Plagiochin E at 2 to 10  $\mu\text{g mL}^{-1}$  was found to enhance the cytotoxicity of adriamycin (drug used to treat breast cancer) against K562/A02 cells by suppressing P-glycoprotein drug transporter activity. This study offers a new chemical candidate to overcome drug resistance in chemotherapy.

In 2010, the same researchers investigated the cytotoxic effects of four natural bisbibenzyls, riccardin C, pakyonol, marchantin M and plagiochin E (Fig. 9) against prostate cancer PC3 cells.<sup>79b</sup>

Bisbibenzyls cytotoxicity against prostate cancer cells is higher than against normal human retina pigment epithelial cells (RPE1) ( $\text{IC}_{50} = 50 \mu\text{M}$ ). By using different tests (flow cytometry assay, typical apoptotic markers (Bcl-2, Bax, caspase-3 PARP) using western blot analysis), these four natural macrocycles were found to induce cell apoptosis with a greater efficiency for marchantin M (Table 15). Each bisbibenzyl induced the strong expression of Bax protein, and a significant decrease of the Bcl-2

expression level. Furthermore, bisbibenzyl-related apoptosis was stopped with the activation of caspase-3 and cleavage of PARP. These data support bisbibenzyls as novel and potent apoptosis inducers for androgen-independent prostate cancer cells.

In terms of the SAR (structure–activity relationship), the OH group and the adjacent oxygen bridge appeared to be the essential features for the inhibitory effects. Indeed riccardin, marchantin M, and plagiochin E induced massive cell death and significant morphological changes at 10  $\mu\text{M}$ , whereas a high dose of pakyonol (20  $\mu\text{M}$ ) was necessary to observe inhibition in cell growth. The interesting results led Lou and co-workers to synthesize brominated and aminomethylated bisbibenzyl analogs in order to improve the cytotoxicity of the natural ones.<sup>80</sup>

The dimethylaminomethylene derivatives **77**, **80a** and **79a** were synthesized from marchantin C, riccardin D and plagiochin E by Mannich reaction, and the derivatives **78a–c**, **80b and c**, and **79b and c** were prepared by bromination with *N*-bromosuccinimide (NBS) (Scheme 14). The most potent cytotoxic effects on three cancer cell lines are presented in Table 16 with  $\text{IC}_{50}$  values.

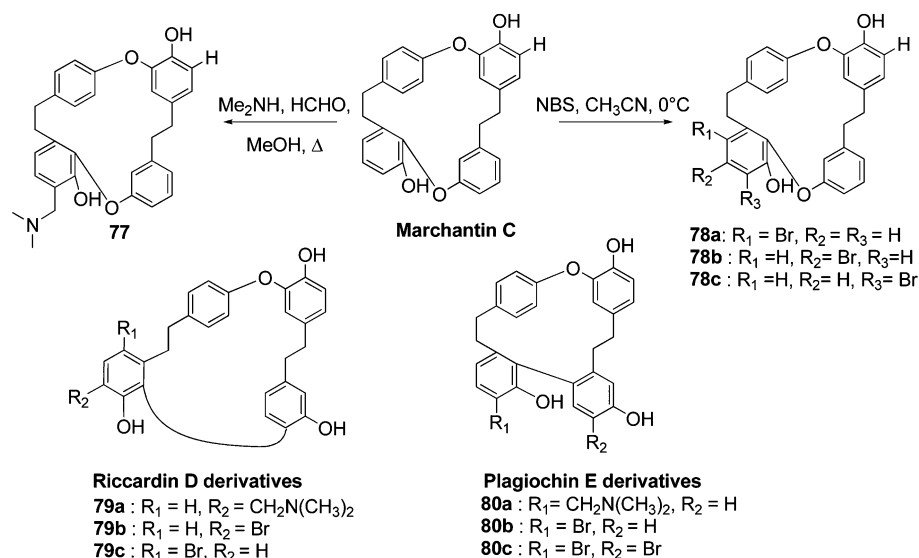
The cytotoxicity of brominated plagiochin E **80b** and **80c** was greatly improved when compared to the parent compound. The dimethylaminomethylene substitution on ring B of riccardin D led to reduced activity (compound **79a**). Riccardin D derivative **79c**, with a bromide substitution on the *para*-position of the hydroxyl group on ring B, was the most cytotoxic compound against KB, MCF-7 and PC3 cell lines, with  $\text{IC}_{50}$  values of 5.9, 5.4 and 5.6  $\mu\text{M}$ , respectively. Analog **79c** effects on cell growth and division were investigated by flow cytometry assay and immunofluorescence microscopic observation. These experiments showed that compound **79c** induced cell cycle arrest at the G2/M phase in a dose-dependent manner as the classical tubulin targeting drugs.<sup>13</sup> The morphological changes in the microtubules network indicated a tubulin depolymerization. Therefore, the bisbibenzyl core is a promising starting point regarding chemical modulation, of great interest to exploit in the search for the discovery of anti-cancer agents. Besides, marchantin C<sup>81</sup> and marchantin A<sup>82</sup> have been studied and demonstrated to be a potent inducer of apoptosis in A172 cell and MCF-7 cells respectively.

Recently, dihydroptychantol A (DHA), another macrocyclic bisbibenzyl compound extracted from liverwort *Asterella angusta*, exhibited multi-drug resistance reversal properties. X. Li and co-workers<sup>83</sup> tested DHA for its anti-cancer activities in human osteosarcoma U2OS cells. DHA induced autophagy followed by apoptosis cell death. Their results have highlighted the potential of the macrocyclic bisbibenzyl core as a good skeleton to design potent anti-tumor agents.

Table 15 Cytotoxic effects and apoptosis induction of four natural bisbibenzyls

Bisbibenzyls	$\text{IC}_{50}^a$ ( $\mu\text{M}$ ) PC3	Apoptotic cells <sup>b</sup> (%)
Riccardin C	3.22	6.21
Pakyonol	7.98	9.40
Marchantin M	5.45	51.62
Plagiochin E	5.99	14.46 0.05 (control)

<sup>a</sup> After 48 h of treatment. <sup>b</sup> Total percent of apoptotic cells resulting from bisbibenzyls treatment at 10  $\mu\text{M}$ .



**Scheme 14** Synthesis of marchantin C, riccardin D and plagiochin E derivatives.

**Table 16** *In vitro* cytotoxicity of three bisbibenzyls and their derivatives in three cancer cell lines KB, MCF-7 and PC3<sup>a</sup>

Bisbibenzyls	IC <sub>50</sub> <sup>b</sup> (μM) KB	IC <sub>50</sub> <sup>c</sup> (μM) MCF-7	IC <sub>50</sub> <sup>d</sup> (μM) PC3
<b>78c</b>	11.3 ± 0.22	12.1 ± 0.14	8.5 ± 0.02
<b>80b</b>	8.2 ± 0.72	6.3 ± 0.69	9.3 ± 0.05
<b>80c</b>	9.7 ± 0.48	8.4 ± 0.09	9.2 ± 0.03
<b>79a</b>	10.7 ± 0.07	13.3 ± 0.21	9.7 ± 0.02
<b>79c</b>	5.9 ± 0.30	5.4 ± 0.07	5.6 ± 0.23
Marchantin C	15.3 ± 0.32	12.8 ± 0.22	5.6 ± 0.23
Riccardin D	7.1 ± 0.11	6.6 ± 0.70	10.1 ± 0.09
Plagiochin E	40.1 ± 1.52	34.9 ± 1.32	28.0 ± 1.86

<sup>a</sup> The IC<sub>50</sub> values (μM) are the concentrations corresponding to 50% inhibition of each cell line. <sup>b</sup> KB, oral cancer cell line. <sup>c</sup> MCF-7, human breast adenocarcinoma cell line. <sup>d</sup> PC3 prostate cancer cell line.

## 4. Conclusion

Drugs used for the treatment of cancer today are essentially cytotoxic (cell-killing). A major challenge is to design new drugs that target specifically cancer cells and at the same time reduce side-effects frequently observed during chemotherapy. For this purpose, over the past decade, the molecular targeted therapies have been developed.<sup>84</sup> Targeted cancer therapies are small chemical molecules which act to block the growth and spread of cancer by interfering with specific molecules essentially proteins involved in tumor growth and progression. That means “molecular anti-cancer targeted therapies” are chemical cytotoxic molecules with a defined biological target. In this way, one could expect to observe less severe side-effects during the anti-cancer treatment that are so common at present. So, all the different processes implicated in the cell division and growth could be a potential therapeutic target to fight cancer. The huge variability of biological targets to discover new anti-cancer drugs and the large diversity of cell lines used to demonstrate an anti-tumor effect make difficult any attempt to rationalize the literature results in this area. Nevertheless, with all the examples cited in this review, we hypothesize that the molecular design using a

diaryl ether core should be a good starting point to discover invaluable new anti-cancer agents. This point of view is reinforced by S. D. Roughley's<sup>85</sup> (2011) analysis on the reactions and frames used during the discovery process of new drug candidates. Diaryl ethers are mentioned, mainly from seven publications from the Pfizer industry, as a “core” to implement. This frame is essentially present in molecules from natural extracts of marine, terrestrial plants or fungi. It could be found implicated in the cyclic structure as in bastadin or marchantin series or in acyclic molecules as in obovatol. This structure difference does not impact the desired biological properties. Moreover, the presence of a halogen substituent on the aromatic ring of a diaryl ether frame, essentially chlorine, bromine or fluoride, seems to increase the tumor cell lines growth inhibition and tubulin polymerization inhibition. The presence of a phenolic hydroxyl group is beneficial for the combrestatin analogs activity and is not interesting for the NF-κB inhibition. Phenolic substances are endowed with both anti- and pro-oxidant properties<sup>86</sup> which could be at the origin of the difference of the results obtained according to the biological target. It is noted that the ADME profiles are up to now missing probably because diaryl ether drugs are not fully explored. Nevertheless we can consider the various advantages of diaryl ether cores in drug design. It is worthy to appreciate how the modulations of the physico-chemical properties by the introduction of different substituents on the aromatic rings save toxicity profile. The easiness and diverse synthetic methods of access as well as the reasonable unexplored medicinal chemistry routes would be worthwhile arguments enough to encourage working with diaryl ether frames. Therefore this justifies the consideration of diaryl ether cores among new anti-cancer candidate research.

## Acknowledgements

We thank Nicolas Ghanty for his useful comments and we also thank the CNRS and the “Université Paul Sabatier” for financial support.

## Notes and references

- 1 A. Jemal, F. Bray, M. M. Center, J. Ferlay, E. Ward and D. Forman, *Ca-Cancer J. Clin.*, 2011, **61**, 69–90.
- 2 R. Krishna and L. D. Mayer, *Eur. J. Pharm. Sci.*, 2000, **11**, 265–283.
- 3 E. Fox, G. A. Curt and F. M. Balis, *Oncologist*, 2002, **7**, 401–409.
- 4 I. Herr and K. M. Debatin, *Blood*, 2001, **98**, 2603–2610.
- 5 K. M. Debatin, *Immunotherapy*, 2004, **53**, 153–159.
- 6 G. I. Evan and K. H. Vousden, *Nature*, 2001, **411**, 342–348.
- 7 C. Y. Wang, M. W. Mayo and A. S. Baldwin Jr, *Science*, 1996, **274**, 784–787.
- 8 J. R. Woodburn, *Pharmacol. Ther.*, 1999, **82**, 241–250.
- 9 V. Rusch, J. Baselga, C. Cordon-Cardo, J. Orazem, M. Zaman, S. Hoda, J. McIntosh, J. Kurie and E. Dmitrovsky, *Cancer Res.*, 1993, **53**, 2379–2385.
- 10 (a) K. Vermeulen, D. R. Van Bockstaele and Z. N. Berneman, *Cell Proliferation*, 2003, **36**, 131–149; (b) D. Goodsell, *Oncologist*, 2003, **8**, 597–598.
- 11 (a) J. Folkman, *Sci. Am.*, 1996, **275**, 150–154; (b) G. Szakács, J. K. Paterson, J. A. Ludwig, C. Booth-Genthe and M. M. Gottesman, *Nat. Rev.*, 2006, **5**, 219–234.
- 12 M. Hidalgo and S. G. Eckhardt, *J. Natl. Cancer Inst.*, 2001, **93**, 178–193.
- 13 J. A. Hadfield, S. Ducki, N. Hirst and A. T. McGown, *Prog. Cell Cycle Res.*, 2003, **5**, 309–325.
- 14 M. A. Jordan and L. Wilson, *Nat. Rev. Cancer*, 2004, **4**, 253–265.
- 15 J. Zhu, *Synlett*, 1997, **2**, 133–144.
- 16 E. N. Pitsinos, V. P. Vidali and E. A. Couladouros, *Eur. J. Org. Chem.*, 2011, 1207–1222.
- 17 (a) Q. Cai, B. Zou and D. Ma, *Angew. Chem., Int. Ed.*, 2006, **45**, 1276–1279; (b) J. F. Marcoux, S. Doye and S. L. Buchwald, *J. Am. Chem. Soc.*, 1997, **119**, 10539–10540.
- 18 C. H. Burgos, T. E. Barder, X. Huang and S. L. Buchwald, *Angew. Chem., Int. Ed.*, 2006, **45**, 4321–4326.
- 19 J. S. Sawyer, *Tetrahedron*, 2000, **56**, 5045–5065.
- 20 (a) M. K. Pyo, Y. Lee and H. S. Yun-Choi, *Arch. Pharm. Res.*, 2002, **25**, 325–328; (b) E. I. Hwang, B. M. Kwon, S. H. Lee, N. R. Kim, T. H. Kang, Y. T. Kim, B. K. Park and S. U. Kim, *J. Antimicrob. Chemother.*, 2002, **49**, 95–101.
- 21 M. S. Choi, S. H. Lee, H. S. Cho, Y. Kim, Y. P. Yun, H. Y. Jung, J. K. Jung, B. C. Lee, H. B. Pyo and J. T. Hong, *Eur. J. Pharmacol.*, 2007, **556**, 181–189.
- 22 S. H. Huang, Y. Chen, P. Y. Tung, J. C. Wu, K. H. Chen, J. M. Wu and S. M. Wang, *J. Cell. Biochem.*, 2007, **101**, 1011–1022.
- 23 S. K. Lee, H. N. Kim, Y. R. Kang, C. W. Lee, H. M. Kim, D. C. Han, J. Shin, K. H. Bae and B. M. Kwon, *Bioorg. Med. Chem.*, 2008, **16**, 8397–8402.
- 24 J. H. Kwak, J. K. In, M. S. Lee, E.-H. Choi, H. Lee, J. T. Hong, Y. P. Yun, S. J. Lee, S. Y. Seo and Y. G. Suh, *Arch. Pharm. Res.*, 2008, **31**, 1559–1563.
- 25 M.-S. Lee, J.-E. Yang, E.-H. Choi, J.-K. In, S. Y. Lee, H. Lee, J. T. Hong, H. W. Lee, Y. G. Suh and J.-K. Jung, *Bull. Korean Chem. Soc.*, 2007, **28**, 1601–1607.
- 26 S. Gupta, K. Hastak, F. Afaq, N. Ahmad and H. Mukhtar, *Oncogene*, 2004, **23**, 2507–2522.
- 27 D. A. Evans, J. L. Katz and T. R. West, *Tetrahedron Lett.*, 1998, **39**, 2937–2940.
- 28 C. Y. Wang, M. W. Mayo, R. G. Korneluk, D. V. Goeddel and A. S. Baldwin Jr, *Science*, 1998, **281**, 1680–1683.
- 29 S. Huneck, *Naturwissenschaften*, 1999, **86**, 559–570.
- 30 S. Huneck, *Fortschr. Chem. Org. Naturst.*, 2001, **81**, 1–276.
- 31 (a) T. Rezanka and I. A. Guschina, *J. Nat. Prod.*, 1999, **62**, 1675–1677; (b) J. A. Elix, J. H. Wardlaw and W. Obermayer, *Aust. J. Chem.*, 2000, **53**, 233–235.
- 32 M. Millot, S. Tomasi, E. Studzinska, I. Rouaud and J. Boustie, *J. Nat. Prod.*, 2009, **72**, 2177–2180.
- 33 P. Chomcheon, S. Wiyakrutta, N. Sriubolmas, N. Ngamrojanavanich, S. Kengtong, C. Mahidol, S. Ruchirawat and P. Kittakoop, *Phytochemistry*, 2009, **70**, 407–413.
- 34 R. W. Brueggemeier, J. C. Hackett and E. S. Diaz-Cruz, *Endocr. Rev.*, 2005, **26**, 331–345.
- 35 D. M. Stresser, S. D. Turner, J. McNamara, P. Stocker, V. P. Miller, C. L. Crespi and C. J. Patten, *Anal. Biochem.*, 2000, **284**, 427–430.
- 36 A. Russo, S. Caggia, M. Piovano, J. Garbarino and V. Cardile, *Chem.-Biol. Interact.*, 2012, **195**, 1–10.
- 37 A. Jemal, R. C. Tiwari, T. Murray, A. Ghafoor, A. Samuels, E. Ward, E. J. Feuer and M. J. Thun, *Ca-Cancer J. Clin.*, 2004, **54**, 8–29.
- 38 O. W. Brawley, S. Barnes and H. Parnes, *Ann. N. Y. Acad. Sci.*, 2001, **952**, 145–152.
- 39 L. W. Wattenberg, J. B. Coccia and A. R. Galbraith, *Cancer Lett.*, 1994, **83**, 165–169.
- 40 I. B. Masesane, S. O. Yeboah, J. Liebscher, C. Muëgge and B. M. Abegaz, *Phytochemistry*, 2000, **53**, 1005–1008.
- 41 L. K. Mdee, S. O. Yeboah and B. M. Abegaz, *J. Nat. Prod.*, 2003, **66**, 599–604.
- 42 H. Zhang, J.-J. Liu, J. Sun, X.-H. Yang, T.-T. Zhao, X. Lu, H.-B. Gong and H.-L. Zhu, *Bioorg. Med. Chem.*, 2012, **20**, 3212–3218.
- 43 (a) J. A. Woods, J. A. Hadfield, G. R. Pettit, B. W. Fox and A. T. McGown, *Br. J. Cancer*, 1995, **71**, 705–711; (b) N. Nguyen-Hai, *Curr. Med. Chem.*, 2003, **10**, 1697–1722.
- 44 G. G. Dark, S. A. Hill, V. E. Prise, G. M. Tozer, G. R. Pettit and D. J. Chaplin, *Cancer Res.*, 1997, **57**, 1829–1834.
- 45 A. Chaudhary, S. N. Pandeya, P. Kumar, P. P. Sharma, S. Gupta, N. Soni, K. K. Verma and G. Bhardwaj, *Mini-Rev. Med. Chem.*, 2007, **7**, 1186–1205.
- 46 N. J. Lawrence, D. Rennison, M. Woo, A. T. McGown and J. A. Hadfield, *Bioorg. Med. Chem. Lett.*, 2001, **11**, 51–54.
- 47 J.-F. Marcoux, S. Doye and S. L. Buchwald, *J. Am. Chem. Soc.*, 1997, **119**, 10539–10540.
- 48 K.-N. Cho and K.-I. Lee, *Arch. Pharm. Res.*, 2002, **25**, 759–769.
- 49 N. M. G. M. Appels, J. H. Beijnen and J. H. M. Schellens, *Oncologist*, 2005, **10**, 565–578.
- 50 S. C. MacTough, S. J. deSolms, A. W. Shaw, M. T. Abrams, T. M. Ciccarone, J. P. Davide, K. A. Hamilton, J. H. Hutchinson, K. S. Koblan, N. E. Kohl, R. B. Lobell, R. G. Robinson and S. L. Graham, *Bioorg. Med. Chem. Lett.*, 2001, **11**, 1257–1260.
- 51 S. J. deSolms, T. M. Ciccarone, S. C. MacTough, A. W. Shaw, C. A. Buser, M. Ellis-Hutchings, C. Fernandes, K. A. Hamilton, H. E. Huber, N. E. Kohl, R. B. Lobell, R. G. Robinson, N. N. Tsou, E. S. Walsh, S. L. Graham, L. S. Beese and J. S. Taylor, *J. Med. Chem.*, 2003, **46**, 2973–2984.
- 52 N. J. Anthony, R. P. Gomez, M. D. Schaber, S. D. Mosser, K. A. Hamilton, T. J. O'Neil, K. S. Koblan, S. L. Graham, G. D. Hartman, D. Shah, E. Rands, N. E. Kohl, J. B. Gibbs and A. I. Oliff, *J. Med. Chem.*, 1999, **42**, 3356–3368.
- 53 R. B. Lobell, C. A. Omer, M. T. Abrams, H. G. Bhimnathwala, M. J. Brucker, C. A. Buser, J. P. Davide, S. J. deSolms, C. J. Dinsmore, M. S. Ellis-Hutchings, A. M. Kral, D. Liu, W. C. Lumma, S. V. Machotka, E. Rands, T. M. Williams, S. L. Graham, G. D. Hartman, D. C. Heimbrook and N. E. Kohl, *Cancer Res.*, 2001, **61**, 8758–8768.
- 54 E. I. Deryugina and J. P. Quigley, *Cancer Metastasis Rev.*, 2006, **25**, 9–34.
- 55 C. K. Wada, J. H. Holms, M. L. Curtin, Y. Dai, A. S. Florjancic, R. B. Garland, Y. Guo, H. R. Heyman, J. R. Stacey, D. H. Steinman, D. H. Albert, J. J. Bouska, I. N. Elmore, C. L. Goodfellow, P. A. Marcotte, P. Tapang, D. W. Morgan, M. R. Michaelides and S. K. Davidsen, *J. Med. Chem.*, 2002, **45**, 219–232.
- 56 M. L. Curtin, A. S. Florjancic, H. R. Heyman, M. R. Michaelides, R. B. Garland, J. H. Holms, D. H. Steinman, J. F. Dellaria, J. A. C. K. Gong, Y. Guo, I. B. Elmore, P. Tapang, D. H. Albert, T. J. Magoc, P. A. Marcotte, J. J. Bouska, C. L. Goodfellow, J. L. Bauch, K. C. Marsh, D. W. Margon and S. K. Davidsen, *Bioorg. Med. Chem. Lett.*, 2001, **11**, 1557–1560.
- 57 G. H. Zayia, *Org. Lett.*, 1999, **1**, 989–991.
- 58 S. N. Raja, B. W. Surber, J. Du and J. L. Cross, *J. Labelled Compd. Radiopharm.*, 2009, **52**, 98–102.
- 59 S. Wilhelm, C. Carter, M. Lynch, T. Lowinger, J. Dumas, R. A. Smith, B. Schwartz, R. Simantov and S. Kelley, *Nat. Rev. Drug Discovery*, 2006, **5**, 835–844.
- 60 M. Sun, X. Wu, J. Chen, J. Cai, M. Cao and M. Ji, *Eur. J. Med. Chem.*, 2010, **45**, 2299–2306.
- 61 V. E. Kuz'min, A. G. Artemenko, R. N. Lozytska, A. S. Fedtchouk, V. P. Lozitsky, E. N. Muratov and A. K. Mescheriakov, *SAR QSAR Environ. Res.*, 2005, **16**, 219–230.
- 62 D. R. Shekawat, S. S. Sabnis and C. V. Deliwala, *J. Med. Chem.*, 1972, **15**, 1196–1197.
- 63 T.-T. Zhao, X. Lu, X.-H. Yang, L.-M. Wang, X. Li, Z.-C. Wang, H.-B. Gong and H.-L. Zhu, *Bioorg. Med. Chem.*, 2012, **20**, 3233–3241.

- 64 G. K. Schwartz, A. Weitzman, E. O'Reilly, L. Brail, D. P. de Alwis, A. Cleverly, B. Barile-Thiem, V. Vinciguerra and D. R. Budman, *J. Clin. Oncol.*, 2005, **23**, 5365–5373.
- 65 M. W. Saif, H. Oettle, W. L. Vervenne, J. P. Thomas, G. Spitzer, C. Visseren-Grul, N. Enas and D. A. Richards, *Cancer J.*, 2009, **15**, 339–343.
- 66 J. Ishida, M. Kozuka, H.-K. Wang, T. Konoshima, H. Tokuda, M. Okuda, X. Y. Mou, H. Nishino, N. Sakurai, K.-H. Lee and M. Nagai, *Cancer Lett.*, 2000, **159**, 135–140.
- 67 M. Karin, Y. Cao, F. R. Greten and Z.-W. Li, *Nat. Rev. Cancer*, 2002, **2**, 301–310.
- 68 B. Farrow and B. M. Evers, *Surg. Oncol.*, 2002, **10**, 153–165.
- 69 W. Y. Jin, X. F. Cai, M. Na, J. J. Lee and K. Bae, *Biol. Pharm. Bull.*, 2007, **30**, 810–813.
- 70 C. V. Bryant, G. D. K. Kumar, A. M. Nyong and A. Natarajan, *Bioorg. Med. Chem. Lett.*, 2012, **22**, 245–248.
- 71 (a) R. Kazlauskas, O. L. Raymond, P. T. Murphy, R. J. Wells and J. F. Blount, *Aust. J. Chem.*, 1981, **34**, 765–786; (b) S. Miao and R. J. Anderson, *J. Nat. Prod.*, 1990, **53**, 1441–1446; (c) G. R. Pettit, M. S. Butler, C. G. Bass, D. L. Doubek, M. D. Williams, J. M. Schmidt, R. K. Pettit, J. N. A. Hooper, L. P. Tackett and M. J. Filiatrault, *J. Nat. Prod.*, 1995, **58**, 680–688; (d) M. S. Butler, T. K. Lim, R. J. Capon and L. S. Hammond, *Aust. J. Chem.*, 1991, **44**, 287–296.
- 72 A. V. Reddy, K. Ravinder, M. Narasimhulu, A. Sridevi, N. Satyanarayana, A. K. Kondapic and Y. Venkateswarlu, *Bioorg. Med. Chem.*, 2006, **14**, 4452–4457.
- 73 H. Greve, S. Kehraus, A. Krick, G. Kelter, A. Maier, H.-H. Fiebig, A. D. Wright and G. M. König, *J. Nat. Prod.*, 2008, **71**, 309–312.
- 74 N. Kotoku, A. Hiramatsu, H. Tsujita, Y. Hirakawa, M. Sanagawa, S. Aoki and M. Kobayashi, *Arch. Pharm. Chem. Life Sci.*, 2008, **341**, 568–577.
- 75 N. Kotoku, H. Tsujita, A. Hiramatsu, C. Mori, N. Koizumi and M. Kobayashi, *Tetrahedron*, 2005, **61**, 7211–7218.
- 76 Y. Asakawa, *Phytochemistry*, 2004, **65**, 623–669.
- 77 C. P. Wu, A. M. Calcagno and S. V. Ambudkar, *Curr. Mol. Pharmacol.*, 2008, **1**, 93–105.
- 78 (a) R. Callaghan, R. C. Ford and I. D. Kerr, *FEBS Lett.*, 2006, **580**, 1056–1063; (b) E. K. Pauwels, P. Erba, G. Mariani and C. M. Gomes, *Drug News Perspect.*, 2007, **20**, 371–377.
- 79 (a) X. Li, B. Sun, C.-J. Zhu, H.-Q. Yuan, Y.-Q. Shi, J. Gao, S.-J. Li and H.-X. Lou, *Toxicol. in Vitro*, 2009, **23**, 29–36; (b) A.-H. Xu, Z.-M. Hu, J.-B. Qu, S.-M. Liu, A. K. A. Syed, H.-Q. Yuan and H.-X. Lou, *Acta Pharmacol. Sin.*, 2010, **31**, 609–615.
- 80 J. Jiang, B. Sun, Y. Wang, M. Cui, L. Zhang, C. Cui, Y. Wanga, X. Liu and H. Lou, *Bioorg. Med. Chem.*, 2012, **20**, 2382–2391.
- 81 Y.-Q. Shi, Y.-X. Liao, X.-J. Qu, H.-Q. Yuan, S. Li, J.-B. Qu and H.-X. Lou, *Cancer Lett.*, 2008, **262**, 173–182.
- 82 W.-J. Huang, C.-L. Wub, Ch.-W. Lin, L.-L. Chi, P.-Y. Chen, C.-J. Chiu, C.-Y. Huang and C.-N. Chen, *Cancer Lett.*, 2010, **29**, 1108–1119.
- 83 X. Li, W. K. K. Wu, B. Sun, M. Cui, S. Liu, J. Gao and H. Lou, *Toxicol. Appl. Pharmacol.*, 2011, **251**, 146–154.
- 84 W. L. Perry and A. Weitzman, *Clin. Adv. Hematol. Oncol.*, 2005, **3**, 199–238.
- 85 S. D. Roughley and A. M. Jordan, *J. Med. Chem.*, 2011, **54**, 3451–3479.
- 86 B. Lipinski, *Oxid. Med. Cell. Longevity*, 2011, **2011**, 1–9.